

# Synthesis, Characterization, and *In Vitro* and *In Vivo* Evaluations of 4-(*N*)-Docosahexaenoyl 2', 2'-Difluorodeoxycytidine with Potent and Broad-Spectrum Antitumor Activity<sup>1,2</sup>

Youssef W. Naguib\*, Dharmika Lansakara-P.\*, Laura M. Lashinger<sup>†</sup>, B. Leticia Rodriguez\*, Solange Valdes\*, Mengmeng Niu\*, Abdulaziz M. Aldayel\*, Lan Peng<sup>‡</sup>, Stephen D. Hursting<sup>§</sup> and Zhengrong Cui\*

\*Pharmaceutics Division, College of Pharmacy, The University of Texas at Austin, Austin, TX 78712;

<sup>†</sup>Department of Nutritional Sciences, College of Natural Sciences, The University of Texas at Austin, Austin, TX 78712; <sup>‡</sup>Department of Pathology, The University of Texas Southwestern Medical Center, Dallas, TX 75390; <sup>§</sup>Gillings School of Global Public Health, University of North Carolina, Chapel Hill, NC 27599

## Abstract

In this study, a new compound, 4-(*N*)-docosahexaenoyl 2', 2'-difluorodeoxycytidine (DHA-dFdC), was synthesized and characterized. Its antitumor activity was evaluated in cell culture and in mouse models of pancreatic cancer. DHA-dFdC is a poorly soluble, pale yellow waxy solid, with a molecular mass of 573.3 Da and a melting point of about 96°C. The activation energy for the degradation of DHA-dFdC in an aqueous Tween 80-based solution is 12.86 kcal/mol, whereas its stability is significantly higher in the presence of vitamin E. NCI-60 DTP Human Tumor Cell Line Screening revealed that DHA-dFdC has potent and broad-spectrum antitumor activity, especially in leukemia, renal, and central nervous system cancer cell lines. In human and murine pancreatic cancer cell lines, the IC<sub>50</sub> value of DHA-dFdC was up to 10<sup>5</sup>-fold lower than that of dFdC. The elimination of DHA-dFdC in mouse plasma appeared to follow a biexponential model, with a terminal phase *t*<sub>1/2</sub> of about 58 minutes. DHA-dFdC significantly extended the survival of genetically engineered mice that spontaneously develop pancreatic ductal adenocarcinoma. In nude mice with subcutaneously implanted human Panc-1 pancreatic tumors, the antitumor activity of DHA-dFdC was significantly stronger than the molar equivalent of dFdC alone, DHA alone, or the physical mixture of them (1:1, molar ratio). DHA-dFdC also significantly inhibited the growth of Panc-1 tumors orthotopically implanted in the pancreas of nude mice, whereas the molar equivalent dose of dFdC alone did not show any significant activity. DHA-dFdC is a promising compound for the potential treatment of cancers in organs such as the pancreas.

*Neoplasia* (2016) 18, 33–48

## Introduction

Docosahexaenoic acid (DHA, 22:6, n-3) is a polyunsaturated fatty acid (PUFA) that has been extensively investigated for its potential antitumor activity, either as a single agent or in combination with other cancer chemotherapeutic agents [1–5]. Omega-3 PUFAs are known to induce apoptosis in various cancer cells [6,7], inhibit cancer cell invasiveness [8], and inhibit metastasis and angiogenesis in tumor tissues [9–11]. The exact mechanism underlying the antitumor activity of omega-3 PUFAs remains unknown, but it is thought to be in part related to its potent antioxidant activity [6]. To better take

Address all correspondence to: Zhengrong Cui, Pharmaceutics Division, College of Pharmacy, The University of Texas at Austin, Austin, TX 78712.

E-mail: [zhengrong.cui@austin.utexas.edu](mailto:zhengrong.cui@austin.utexas.edu)

<sup>1</sup> This work was supported in part by grants from the U.S. National Institutes of Health (CA179362 and CA135274) to Z. C. Y. W. N. was supported by a doctoral scholarship from the Egyptian Ministry of Higher Education.

<sup>2</sup> Conflict of interest: None.

Received 11 August 2015; Revised 11 November 2015; Accepted 11 November 2015

© 2015 The Authors. Published by Elsevier Inc. on behalf of Neoplasia Press, Inc. This is an open access article under the CC BY-NC-ND license (<http://creativecommons.org/licenses/by-nc-nd/4.0/>).

1476-5586/15  
<http://dx.doi.org/10.1016/j.neo.2015.11.012>

advantage of the antitumor activity of DHA, it was previously conjugated with some commonly used cancer chemotherapeutic agents, such as paclitaxel, doxorubicin, and camptothecin [12–14]. For example, Bradley et al. showed that conjugation of DHA to paclitaxel significantly modified the pharmacokinetics and biodistribution of paclitaxel, prompting the testing of the DHA-paclitaxel conjugate (i.e., Taxoprexin) in clinical trials [14–16], although the DHA-paclitaxel conjugate was not more cytotoxic than paclitaxel alone against many tumor cells in culture [14,17,18].

Gemcitabine HCl (2', 2'-difluorodeoxycytidine HCl, dFdC) is a fluorinated deoxycytidine analogue. It is one of the standard treatments of locally advanced and metastatic pancreatic cancer [19,20] and is also used in combination therapy of other solid tumors including breast, bladder, lung, and ovarian cancers [19,21,22]. Extensive deamination at the 4-amino site, which takes place both intracellularly and extracellularly by the action of cytidine deaminase, is responsible for the loss of about 90% of dFdC after intravenous administration, and the deaminated metabolite difluorodeoxyuridine is almost inactive [19,23–26]. More than 99% of administered dFdC is excreted in the urine, with unchanged dFdC comprising only 5% [19,27]. Over the years, there have been reports showing that chemical modifications of this fluorinated deoxycytidine analogue may potentially improve its efficacy and/or safety profiles. For example, it was shown that conjugation of a fatty acid, such as stearic acid, to dFdC at the 4-NH<sub>2</sub> group decreases the sensitivity of the latter to deaminase; modifies its pharmacokinetics; and, in some cases, improves its *in vivo* antitumor activity [24,28–41].

In the present study, we report the synthesis, characterization, and *in vitro* and *in vivo* evaluations of 4-(*N*)-docosahexaenoyl 2', 2'-difluorodeoxycytidine (DHA-dFdC) conjugate. DHA-dFdC showed potent and broad spectrum antitumor activity in various human cancer cell lines in culture. DHA-dFdC also showed an unexpectedly longer residence time in mouse pancreas compared with dFdC. Because pancreatic cancer is one of the most aggressive, and in most cases fatal, types of cancer, with a mortality rate almost equal to incidence rate [42,43], the antitumor activity of the DHA-dFdC was primarily evaluated in mouse models of pancreatic cancer.

## Materials and Methods

### Materials

Gemcitabine HCl (dFdC) was from Biotang, Inc. (Lexington, MA). Cis-4,7,10,13,16,19-docosahexaenoic acid (DHA), 1-(3-dimethylaminopropyl)-3-ethylcarbodiimide HCl and trifluoroacetic acid (TFA) were from Acros Organics (Morris Plains, NJ). Di-tert-butyl-dicarbonate, 3-(4,5-dimethylthiazol-2-yl)-2,5-diphenyltetrazolium bromide (MTT), vitamin E, HPLC-grade methanol, sodium dodecyl sulfate (SDS), Triton X-100, and Tween 80 were from Sigma-Aldrich (St. Louis, MO). Hydroxy-7-azabenzotriazole was from CreoSalus, Inc. (Louisville, KY). Isopropyl myristate (IPM) was from TCI America (Montgomeryville, PA). Anhydrous sodium sulfate, ammonium chloride, mono- and di-basic sodium phosphates, ethyl acetate, HPLC-grade acetonitrile, dichloromethane (DCM), acetone, hexane, and octanol were from Thermo Fisher (Waltham, MA). BD Matrigel Basement Membrane Matrix was from BD Biosciences (San Jose, CA). D-Luciferin K<sup>+</sup> salt bioluminescent substrate was from Perkin Elmer (Waltham, MA). Guava Nexin reagent for flow cytometry was from EMD Millipore (Billerica, MA). Lactate dehydrogenase (LDH) cytotoxicity detection kit was from Takara-Clontech Laboratories, Inc. (Mountain View, CA). Dulbecco's modified Eagle medium (DMEM), Roswell Park Memorial Institute (RPMI 1640)

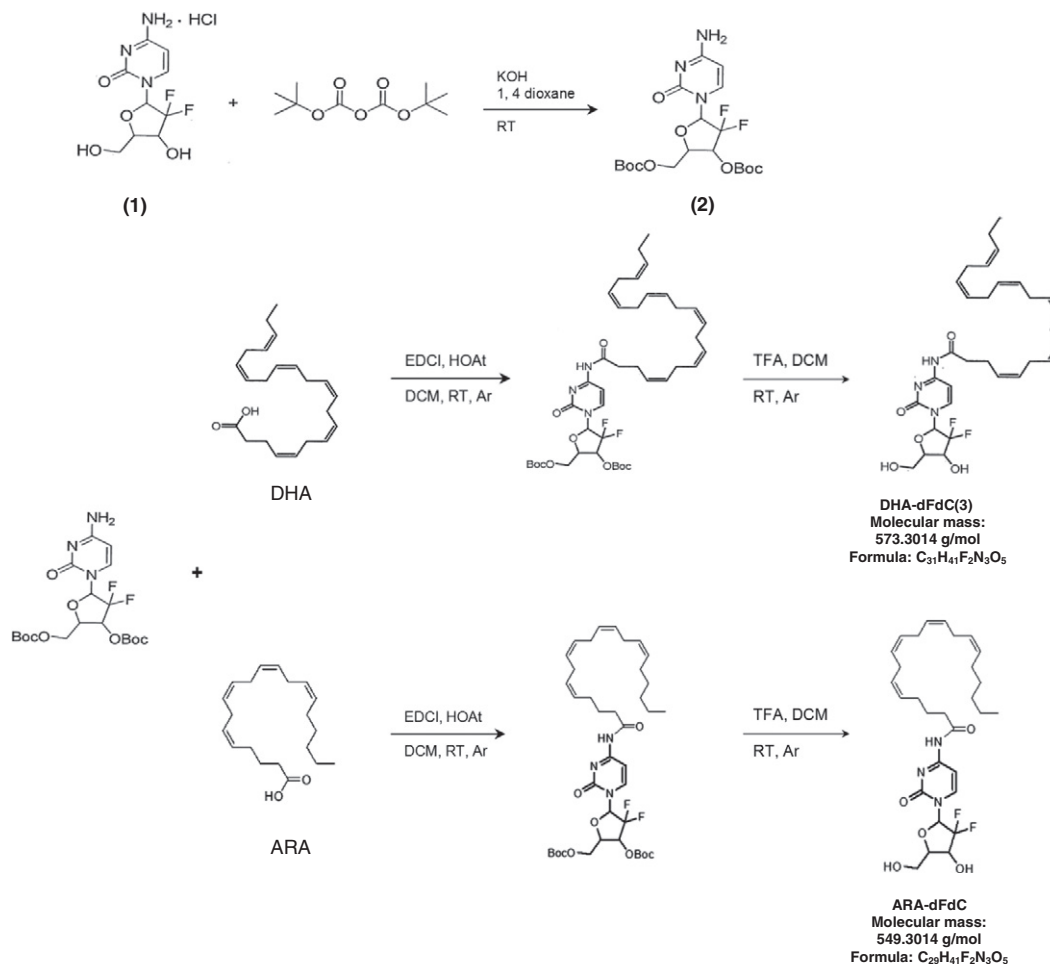
medium, fetal bovine serum (FBS), penicillin, streptomycin, horse serum, and Dulbecco's phosphate buffer saline were all from Invitrogen-Life Technologies (Carlsbad, CA). All other chemicals, reagents, and solvents were of analytical grade and used as received without further purification.

### Cell Lines

Panc-02 (mouse pancreatic cancer cell line), BxPC-3 (human pancreatic cancer cell line), MIA PaCa-2 (human pancreatic cancer cell line), and TC-1 (mouse lung cancer cell line) were from the American Type Culture Collection (ATCC, Manassas, VA). Panc-1-luc human pancreatic cancer cell line was generously provided by Dr. Dawn E. Quelle at the University of Iowa [44]. TC-1 and Panc-02 cells were grown in RPMI 1640 medium. BxPC-3, MIA PaCa-2, and Panc-1-luc cells were grown in DMEM. All media were supplemented with 10% FBS, 100 U/ml of penicillin, and 100 g/ml of streptomycin, and the DMEM for MIA PaCa-2 cells was supplemented additionally with 2.5% horse serum.

### Synthesis of DHA-dFdC

DHA-dFdC was synthesized following a previously reported conjugation scheme with slight modifications [24,25,29] (Scheme 1). Briefly, dFdC (**1**) (200 mg, 0.67 mmol) in 13.3 ml of 1 N potassium hydroxide was cooled to 4°C. To this solution, di-tert-butyl dicarbonate (Boc<sub>2</sub>O, 1.483 g, 6.8 mmol) in 13.3 ml of anhydrous dioxane was added over 10 minutes under argon atmosphere as previously reported [45]. The reaction mixture was stirred at room temperature (~22°C) for 1 hour and extracted with ethyl acetate (EtOAc). The organic layer was washed with brine, dried over anhydrous sodium sulfate (Na<sub>2</sub>SO<sub>4</sub>), and filtered. Solvent was removed under reduced pressure. The residue was added to Boc<sub>2</sub>O (1.483 g, 6.8 mmol) in 13.3 ml of anhydrous dioxane and 13.3 ml of 1 M KOH at room temperature. The reaction was monitored by thin-layer chromatography. After 1 hour, the reaction mixture was extracted to EtOAc. The organic layer was washed with brine, dried over anhydrous Na<sub>2</sub>SO<sub>4</sub>, and filtered. Solvent was then removed, and the crude product was purified by column chromatography (DCM to acetone, 1:1, v/v). The desired product fractions were pooled and dried to yield 219 mg (71%) of 3',5'-O-bis(tert-butoxycarbonyl) dFdC (**2**). <sup>1</sup>H nuclear magnetic resonance (NMR) (500 MHz, acetone-d<sub>6</sub>) δ 7.60 (1 H, d, J = 7.6 Hz, 6-CH), 6.34 (1 H, brs, 1'-CH), 5.97 (1 H, d, J = 7.6 Hz, 5-CH), 5.29 (1 H, brs, 3'-CH), 4.53–4.39 (3 H, m, 4'-CH, 5'A-CH, 5'B-CH), 2.82 (2 H, s, NH<sub>2</sub>), 1.50, 1.47 (18 H, two s, (CH<sub>3</sub>)<sub>3</sub>C). A solution that contains 3',5'-O-bis(tert-butoxycarbonyl) dFdC (150 mg, 324 μmol), DHA (123 mg, 373.9 μmol), and hydroxy-7-azabenzotriazole (75 mg, 551.1 μmol) in anhydrous DCM was precooled to 4°C, and 1-(3-dimethylaminopropyl)-3-ethylcarbodiimide HCl (93.75 mg, 604.1 μmol) was added. The mixture was degassed by vacuum sonication and then stirred at room temperature under argon for about 40 hours. Water (5 ml) was added to the reaction mixture and extracted three times with a mixture of EtOAc and hexane (2:1, v/v). The combined organic phase was washed with saturated ammonium chloride (NH<sub>4</sub>Cl) and brine and then dried over anhydrous Na<sub>2</sub>SO<sub>4</sub>. The solvent was evaporated, and the residue was purified by column chromatography (EtOAc to hexane, 3:7, v/v). The conjugated amide was isolated and quantified (~165 mg). <sup>1</sup>H NMR was as follows: (300 MHz, acetone-d<sub>6</sub>) δ 9.18 (1 H, s, NHCO), 7.83 (1 H, d, J = 7.8 Hz, 6-CH), 7.49 (1 H, d, J = 7.8 Hz, 5-CH), 6.47–6.42 (1 H, m, 1'-CH), 5.42–5.30 (12 H, m, CH<sub>2</sub>), 5.30–5.05 (1 H, m, 3'-CH), 4.50–4.34 (3 H, m, 4'-CH and 5'-CH), 2.90–2.79 (10 H, m, CH<sub>2</sub>), 2.60–2.40



**Scheme 1.** Synthesis of DHA-dFdC and ARA-dFdC. RT, room temperature; Ar, argon.

(4 H, m, CH<sub>2</sub>), 2.07 (2 H, p, J = 7.5 Hz, CH<sub>2</sub>), 1.53-1.46 (18H, m, (CH<sub>3</sub>)<sub>3</sub>C), 0.97 (3 H, t, J = 7.4 Hz, terminal CH<sub>3</sub>). To a stirred solution of the conjugated amide (37 mg, 47.8 nmol) in 3 ml of DCM, about 0.2 ml of TFA was added. This solution was stirred at room temperature for 4 hours, and excess TFA was removed under reduced pressure. The concentrated sample was codistilled with DCM for three times. The crude sample was chromatographed on silica gel (DCM to ethanol, 94:6, v/v) [25,28]. The desired fractions were pooled, and the solvent was evaporated to yield 4-(*N*)-DHA-dFdC (**3**) (DHA-dFdC, ~80 mg, ~36% of original combined weights of dFdC and DHA), which appeared as a pale yellow dry waxy solid. <sup>1</sup>H NMR (300 MHz, THF-d<sub>4</sub>) was as follows: δ 10.13 (1H, s, NHCO), 8.17 (1H, d, J = 7.5 Hz, 6-CH), 7.37 (1H, d, J = 7.5 Hz, 5-CH), 6.25 (1H, t, J = 7.4 Hz, 1'-CH), 5.51-5.27 (12H, m, CH), 4.40-4.20 (1H, m, 3'-CH), 3.95-3.70 (3H, m, 4'-CH and 5'-CH), 2.95-2.82 (10H, m, CH<sub>2</sub>), 2.50-2.41 (4H, m, CH<sub>2</sub>), 2.08 (2H, p, J = 7.2 Hz, CH<sub>2</sub>), 0.96 (3H, t, J = 7.7 Hz, terminal CH<sub>3</sub>) (see Figure S1A in the Supplement for <sup>1</sup>H NMR spectrum). ESI-HRMS [M + Na]<sup>+</sup> *m/z* calculated for C<sub>31</sub>H<sub>41</sub>F<sub>2</sub>N<sub>3</sub>NaO<sub>5</sub> is: 596.29065, found: 596.29068. The purity of the synthesized compound was confirmed by LC/mass spectrometry (MS) following gradient elution (Figure S1, B and C, Supplement).

The 4-(*N*)-arachidonyl dFdC (ARA-dFdC) was synthesized similarly, except that the DHA was replaced with arachidonic acid (ARA), an omega-6 PUFA (Scheme 1). The structure of the resultant ARA-dFdC was confirmed using <sup>1</sup>H NMR and MS (data not shown).

### Determination of the Solubility and Partition Coefficient of DHA-dFdC

The aqueous solubility of DHA-dFdC was determined following an indirect method according to Beall et al. with minimal modifications [46]. Briefly, excess amount of DHA-dFdC was added to 100 μl of IPM in crimp-sealed amber glass vials under nitrogen and was stirred vigorously at room temperature for 24 hours, protected from light. After the stirring was stopped, the mixture was left to stand for an additional 24 hours for equilibration. The content of the vial was centrifuged (14,000 rpm, 10 minutes), and the supernatant was transferred into a different tube. Aliquots of the saturated IPM solution were used to measure the DHA-dFdC concentration before partitioning (A<sub>1</sub>) using HPLC (after proper dilution with methanol). The HPLC method will be discussed in details later. Then, water was added to the IPM saturated solution in a volume ratio of 10:1. The two phases were mixed by vortexing for 5 minutes, left to stand for 15 minutes, and then centrifuged (14,000 rpm, 15 minutes) to collect the IPM layer. DHA-dFdC concentration in the IPM layer (A<sub>2</sub>) was again measured using HPLC after partitioning. The following equation was used to calculate the partition coefficient (K<sub>IPM/water</sub>) [46]:

$$K_{\text{IPM/water}} = [A_1 / (A_1 - A_2)] \times [V_{\text{water}} / V_{\text{IPM}}] \quad (1)$$

Where *V*<sub>water</sub> is the volume of the water phase and *V*<sub>IPM</sub> is the volume of IPM, and the value of *V*<sub>water</sub>/*V*<sub>IPM</sub> was 10.

The aqueous solubility ( $S_w$ ) of DHA-dFdC was determined using the following equation [46]:

$$S_w = S_{IPM}/K_{IPM/water} \quad (2)$$

Where  $S_{IPM}$  is the solubility of DHA-dFdC in IPM, and DHA-dFdC was found to be stable in IPM under test conditions for at least 48 hours.

The octanol-water partition coefficient of DHA-dFdC was determined using a previously reported method with minor modifications [47]. Briefly, octanol and PBS (7.4, 0.01 M) were mutually saturated for 24 hours. DHA-dFdC was dissolved in octanol (0.4 mg/ml, PBS-saturated), and 10  $\mu$ l of the solution was withdrawn and diluted with methanol to measure DHA-dFdC concentration using HPLC ( $C_1$ ). PBS was added to octanol at a volume ratio ( $V_{PBS}/V_{oct}$ ) of 20:1 into a sealed vial under nitrogen, and the mixture was agitated vigorously at room temperature using a horizontal orbital shaker at 250 rpm (Max Q 2000, Thermo Scientific) while protected from light. After 5 hours, the mixture was centrifuged (14,000 rpm, 15 minutes), and the concentration of DHA-dFdC in the octanol layer was determined using HPLC ( $C_2$ ). Partition coefficient ( $K_{oct/water}$ ) was calculated using the following equation:

$$K_{oct/water} = [C_1/(C_1 - C_2)] \times [V_{PBS}/V_{oct}] \quad (3)$$

DHA-dFdC was found to be stable in octanol under the test conditions for at least 18 hours (data not shown).

#### Chemical Stability of DHA-dFdC in an Aqueous Solution

DHA-dFdC is freely soluble in ethanol and in Tween 80. It was solubilized into a formulation that contains Tween 80, ethanol, and water (volume ratio, 1:0.52:8.48) to evaluate its *in vivo* activity. The stability of DHA-dFdC in this formulation was evaluated in crimp-sealed amber glass vials under nitrogen atmosphere. Briefly, 150  $\mu$ l of the DHA-dFdC aqueous solution at a concentration of about 7 mg/ml was added to the amber glass vials under nitrogen atmosphere, and the vials were crimp-sealed with aluminum seals over rubber lids. At predetermined time intervals, 10  $\mu$ l of the solution was diluted with 90  $\mu$ l of methanol and mixed, and the concentration was measured using HPLC. Stability tests were carried out at room temperature ( $\sim 22^\circ\text{C}$ ) or  $4^\circ\text{C}$  in triplicates. Vitamin E was added in the formulation to a final concentration of 0.01% or 0.04% (v/v) to evaluate the effect of vitamin E on the chemical stability of DHA-dFdC.

To study the effect of temperature on the chemical stability of DHA-dFdC, the DHA-dFdC formulation in crimp-sealed vials under nitrogen was stored at room temperature,  $37^\circ\text{C}$ , or  $60^\circ\text{C}$ , protected from light. Sampling and analyses were carried out at predetermined time points as described above. The first-order degradation reaction equation was used to calculate the values of the reaction rate constant ( $k$ ) at different temperatures. Arrhenius plot was constructed by plotting the  $\log k$  values versus  $1/T$  to calculate the activation energy ( $E_a$ , in kcal/mol) [48].

#### Physicochemical Characterizations of DHA-dFdC

The UV-Vis absorbance of DHA-dFdC, DHA, dFdC, and the physical mixture of dFdC and DHA, all dissolved in methanol, was evaluated using a BioTek Synergy HT Multi-Mode Microplate Reader (Winooski, VT) using the scanning mode. Modulated differential scanning calorimetry (DSC) was used to evaluate the thermal

properties of DHA-dFdC. Samples (2–4 mg) were placed in sealed pans, and the DSC analysis was carried out using DSC Q200 (TA Instruments, New Castle, DE) at a ramp rate of  $5^\circ\text{C}/\text{min}$  under nitrogen flow. X-ray diffraction (XRD) analyses of DHA-dFdC, dFdC, DHA, and the physical mixture of dFdC and DHA (1:1, m/m) was carried out in the x-ray facility in the Department of Chemistry at the University of Texas at Austin using a Rigaku Spider single-crystal x-ray diffractometer (Rigaku, Tokyo, Japan).

#### Evaluation of the Cytotoxicity of DHA-dFdC in Tumor Cells in Culture

The cytotoxicity DHA-dFdC was tested using the NCI-60 DTP Human Tumor Cell Line Screen service (<http://dtp.nci.nih.gov/branches/btb/ivclsp.html>). The NCI-60 cell lines do not include any pancreatic cancer cell lines. Therefore, DHA-dFdC was also evaluated in mouse (Panc-02) and human (Panc-1-luc, and BxPC-3) pancreatic cancer cell lines. TC-1 is a mouse lung cancer cell line that grows aggressively in mice [24]. The cytotoxicity of DHA-dFdC was also evaluated in TC-1 cells. For TC-1, Panc-02, BxPC-3, and Panc-1-luc cells, cells (1500/well for Panc-02, BxPC-3, and Panc-1-luc, and 3000/well for TC-1) were seeded in 96-well plates and incubated at  $37^\circ\text{C}$  and 5%  $\text{CO}_2$  overnight. The cells were then treated with various concentrations of DHA-dFdC, dFdC, DHA, or physical mixture of dFdC and DHA (i.e., DHA + dFdC, 1:1 molar ratio) for 24 hours for Panc-1-luc and TC-1, 48 hours for Panc-02, and 72 hours for BxPC-3. Cell survival was determined using an MTT assay as previously described [49]. DHA-dFdC, DHA, and DHA and dFdC mixture were dissolved in dimethyl sulfoxide (DMSO), whereas dFdC was dissolved in cell culture media. In a separate experiment, Panc-02 cells were also treated for 4 hours with higher concentrations of DHA-dFdC (i.e., 10–100  $\mu\text{M}$ ) or molar equivalent concentrations of dFdC, DHA, or dFdC + DHA (1:1 m/m), and cytotoxicity was measured using MTT assay. The cytotoxic activity of DHA-dFdC in Panc-02 cells was also evaluated using an LDH assay kit. Briefly, Panc-02 cells (1500 cells/well) were seeded in 96-well plates and incubated at  $37^\circ\text{C}$  and 5%  $\text{CO}_2$  for 24 h, followed by treatment with DHA-dFdC or dFdC as mentioned above for 48 hours. LDH activity in the cell culture medium was determined following the manufacturer's instruction. Finally, the cytotoxicity of the ARA-dFdC was also evaluated in MIA PaCa-2 and BxPC-3 cells using MTT assay (1000 cells/well, 72 hours of treatment) as mentioned above. The values of  $\text{IC}_{50}$  were calculated using either GraphPad Prism (GraphPad software, Inc., La Jolla, CA) or Microsoft Excel.

Apoptosis analysis was carried out as previously reported [50]. Briefly, 100,000 Panc-02 cells were incubated in 24-well plates for 24 hours at  $37^\circ\text{C}$  and 5%  $\text{CO}_2$  and then coincubated with various concentrations of DHA-dFdC for 48 hours. Cells were then harvested and stained with 0.1 ml of Guava Nexin reagent (Millipore Corporation, Billerica, MA) for 20 minutes at room temperature, protected from light. The stained cells were analyzed using a Millipore Guava EasyCyte 8HT Flow Cytometry System. Control cells were left untreated.

#### Cellular Uptake of dFdC

The uptake of DHA-dFdC by Panc-02 cells was evaluated. Briefly, 250,000 cells were seeded in 12-well plates and incubated overnight, followed by the addition of DHA-dFdC (or dFdC as a control) to a final concentration of 10  $\mu\text{M}$ . Four hours later, the medium was removed, and cells were lysed using 500  $\mu$ l of 1:1 mixture of 2% SDS



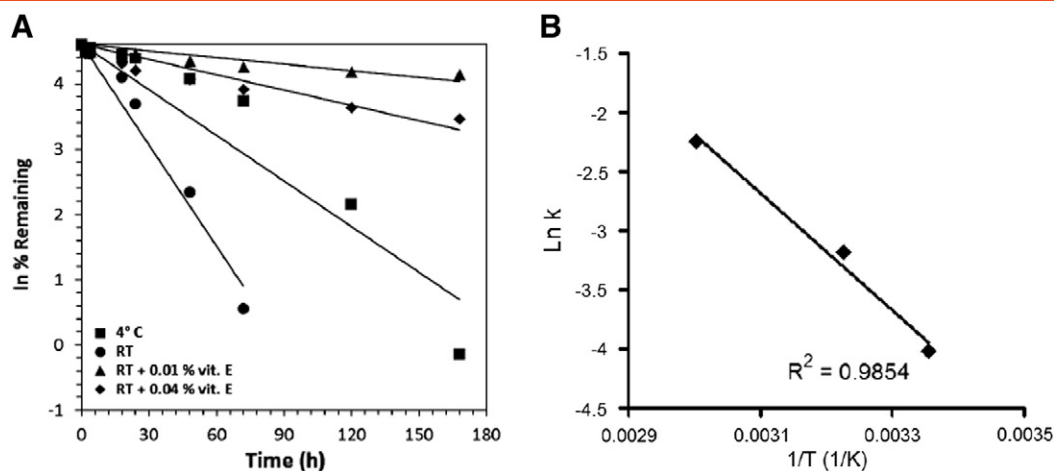


**Figure 1.** Chemical stability of DHA-dFdC. (A) The concentration-time curves of DHA-dFdC at room temperature ( $\sim 22^{\circ}\text{C}$ ) in a solution (i.e., Tween 80/ethanol/water) that contained 0%, 0.01%, or 0.04% (v/v) of vitamin E. As a control, the stability at  $4^{\circ}\text{C}$  is also shown. (B) Arrhenius plot showing the effect of temperature on the rate constant of the degradation of DHA-dFdC in a Tween 80/ethanol/normal saline solution. Data shown are mean from at least three repeats, and standard deviations were not shown for clarity.

and 1% Triton X for 15 minutes at room temperature. The cell lysate was centrifuged (14,000 rpm, 10 minutes) to collect supernatant, which was used for protein assay using Pierce BCA protein assay kit (Life Technologies, Carlsbad, CA). For cells that were incubated with dFdC, before the centrifugation of the cell lysate, tetrahydrouridine (4  $\mu\text{l}$  of 10 mg/ml in water) was added into the cell lysate to inhibit deamination, and deoxyuridine (20  $\mu\text{l}$  of 20  $\mu\text{g}/\text{ml}$  in water) was added as an internal standard. DHA-dFdC was extracted from the cell lysate using ethyl acetate, which was evaporated under nitrogen, and the residue was redissolved in 100  $\mu\text{l}$  of methanol and analyzed by HPLC. To extract dFdC, the cell lysate was mixed with acetonitrile for protein precipitation, followed by centrifugation and collection of the supernatant, which was evaporated under air stream at  $45^{\circ}\text{C}$ . The residue was redissolved in 200  $\mu\text{l}$  of water and analyzed using HPLC. Standard curves were constructed using various concentrations of DHA-dFdC or dFdC in cell lysates.

### Pharmacokinetics and Biodistribution of DHA-dFdC

Animal protocols were approved by the Institutional Animal Care and Use Committee at the University of Texas at Austin. Healthy female C57BL/6 mice (6–8 weeks, Charles River Laboratories, Wilmington, MA) were injected intravenously (IV) with DHA-dFdC in Tween 80/ethanol/water (with 5% mannitol) solution at the dose of 75 mg/kg. At various time points (5, 15, 30, 60, 120, and 180 minutes), 3 mice were euthanized to collect blood. DHA-dFdC was extracted from plasma using ethyl acetate and analyzed using HPLC. Data were analyzed using the Pharsight WinNonlin software (Sunnyvale, CA). Pancreatic DHA-dFdC levels were evaluated in healthy female BALB/c mice (17–20 weeks old, Charles River) following IV injection of the mice with DHA-dFdC in a Tween 80/ethanol/5% mannitol aqueous solution (75 mg/kg). At various time points (i.e., 5, 30, 60, 90, 180, and 300), mice were euthanized ( $n = 3$ –4 per time point). The pancreas was collected and homogenized, and DHA-dFdC was extracted using ethyl acetate and analyzed using HPLC. As a control, the content of dFdC in mouse pancreas was also measured at various time points after mice were IV injected with dFdC (75 mg/kg in 5% mannitol solution). Before extraction of dFdC, tetrahydrouridine was added as a deoxycytidine deaminase inhibitor,

deoxyuridine was added as an internal standard, and dFdC was quantified using HPLC, as previously reported with modification [51]. The area under the DHA-dFdC pancreatic level curve was calculated and compared with that of dFdC using the PKSolver following a noncompartmental model and extravascular administration [52].

### HPLC

HPLC analysis of DHA-dFdC was performed using an Agilent Infinity 1260 (Agilent Corp., Santa Clara, CA) with a RP-C18 column (Zorbax Eclipse, 5  $\mu\text{m}$ , 4.5 mm  $\times$  150 mm, Santa Clara, CA). The mobile phase was methanol and water (90:10, v/v). The flow rate was 1.0 ml/min, and the detection wavelength and injection volume were 248 nm and 5  $\mu\text{l}$ , respectively. When cell lysate, mouse plasma, or tissue samples were used, the mobile phase was methanol and 1% (v/v) acetic acid in water (85:15, v/v) with a flow rate of 1.2 ml/min and injection volume of 20  $\mu\text{l}$ . When DHA-dFdC levels were assayed in pancreatic tissues, the detection wavelength was 300 nm. The concentration of dFdC was determined using a previously reported method with modifications [51]. Briefly, an Agilent 1260 Infinity HPLC Station equipped with a RP-C18 column (Zorbax Eclipse, 5  $\mu\text{m}$ , 3 mm  $\times$  150 mm) at a controlled temperature of  $20^{\circ}\text{C}$ , an Agilent quaternary pump, and an Agilent Diode array UV detector was used. The mobile phase was composed of solution A (phosphate buffer, pH adjusted to 3.0 using phosphoric acid) and solution B (acetonitrile). The column was equilibrated using solution A for at least 30 minutes at a flow rate of 0.6 ml/min followed by another 30 minutes at 1.2 ml/min. The gradient elution consisted of 100% solution A for 6 minutes followed by a gradual change to 97% solution A and 3% solution B over 1 minute. This composition was maintained for 2 minutes, and the composition was returned back to 100% solution A over 1 minute. Between runs, the column was rinsed with methanol:water (90:10, v/v) and methanol:water (50:50, v/v), each for about 15 minutes, and then equilibrated with solution A. The flow rate was 1.2 ml/min. The detection wavelength was 276 nm.

### Evaluation of the Antitumor Activity of DHA-dFdC in Animal Models

*Transgenic mice with spontaneously developed pancreatic tumors.* Female Kras Ink4a<sup>+/-</sup> mice bred in the Animal Research Center at the

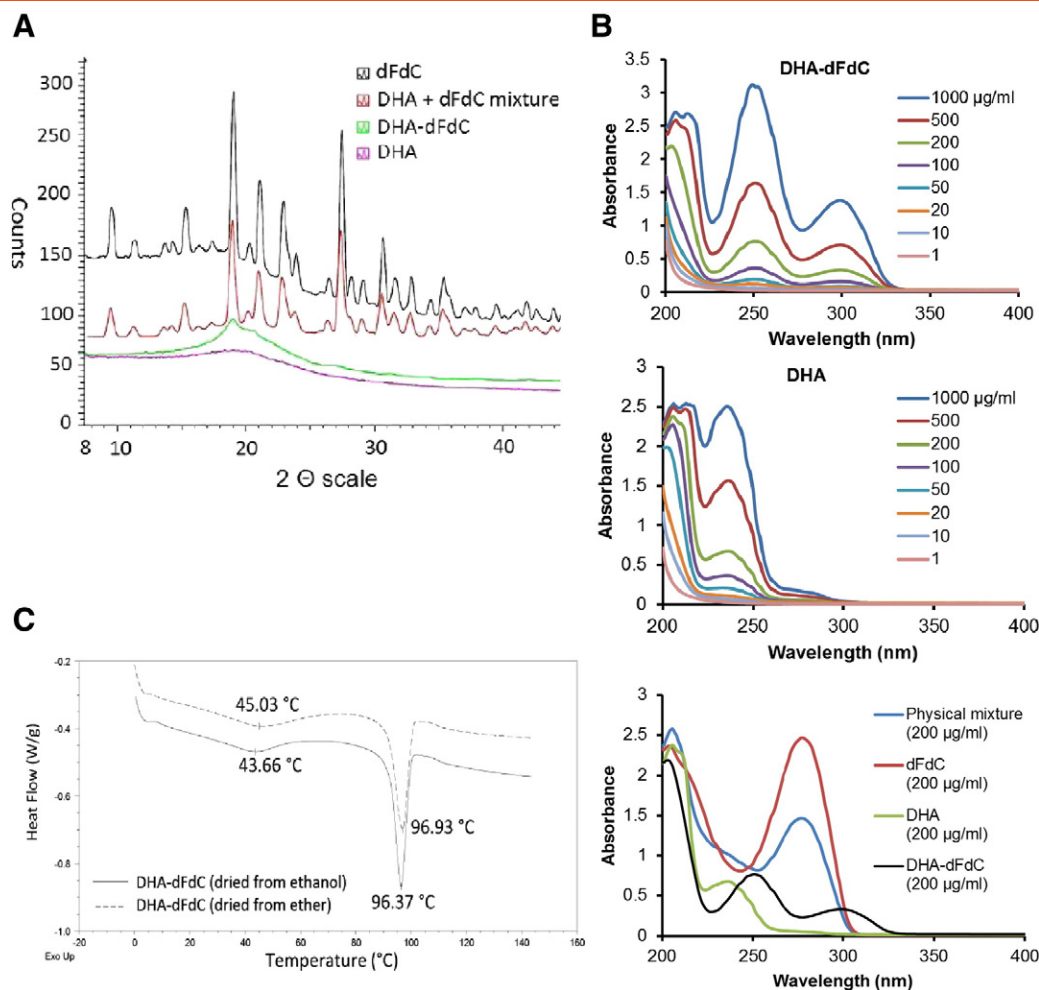


**Figure 2.** (A) XRD patterns of DHA-dFdC, dFdC, DHA, and the mixture of dFdC and DHA (i.e., DHA + dFdC, 1:1, m/m). (B) UV/Vis spectra of DHA-dFdC and DHA at various concentrations, and a comparison of the UV/Vis spectra of DHA-dFdC, dFdC, DHA, and DHA + dFdC physical mixture. (C) DSC analyses of DHA-dFdC precipitated from ethanol solution (solid line) or ether (dashed line).

University of Texas at Austin were used [53]. Kras Ink4a<sup>+/-</sup> mice spontaneously develop pancreatic tumors that resemble human pancreatic tumors [53]. To accelerate pancreatic tumor development, mice were transferred to a special diet (D1249, 60% kcal fat; Research Diets, Inc., New Brunswick, NJ) at the age of 16 weeks [53]. Starting at the age of 20 weeks, mice were grouped and treated with DHA-dFdC [ $n = 5$ , 50 mg/kg, intraperitoneal (IP) injection, up to twice a week for total of 29 doses] or left untreated ( $n = 6$ ), and their health and survival were monitored. In another experiment, female Kras Ink4a<sup>+/-</sup> mice that were placed on the special high fat diet at 10 to 12 weeks of age were randomized into 2 groups ( $n = 6$ ) at the age of 19 to 20 weeks and were either treated with DHA-dFdC (65 mg/kg, IP, twice a week) or left untreated until week 30. Mice were then euthanized, and their pancreas were collected, fixed in formalin, and embedded in paraffin blocks for histological evaluation.

**Mice with subcutaneous Panc-1-luc tumors.** Male athymic nude mice (6–8 weeks, Charles River) were subcutaneously (SC) injected with Panc-1-luc cells ( $5 \times 10^6$  cells in a DMEM and Matrigel mixture, 1:1 v/v). When tumors reached 5 to 7 mm, mice were randomized into 5 groups ( $n = 5$ –6) and injected with DHA-dFdC (IP, 50 mg/kg, or  $\sim 0.087$  mol/kg,  $n = 6$ ), dFdC (26.1 mg/kg, or

$\sim 0.087$  mol/kg,  $n = 6$ ), DHA (28.7 mg/kg, or  $\sim 0.087$  mol/kg,  $n = 5$ ), or the physical mixture of dFdC (26.1 mg/kg) and DHA (28.7 mg/kg) ( $n = 6$ ). DHA-dFdC, DHA alone, and the mixture of DHA and dFdC were dissolved in Tween 80/ethanol/water at a ratio of 1:0.52:8.48 with 5% w/v mannitol, whereas dFdC alone was dissolved in 5% w/v of mannitol solution. As a vehicle control, mice were also injected with the Tween 80/ethanol-based solution alone ( $n = 6$ ). Treatments were repeated twice a week for up to six times, and tumor growth was monitored using a digital caliper. Tumor volumes ( $V$ ) were calculated based on the longest diameter ( $L_1$ ) and the shortest diameter ( $L_2$ ) of each tumor using the equation of  $V = \frac{1}{2} \times L_1 \times L_2 \times L_2$  [54].

**Mice with orthotopic Panc-1-luc tumors.** Panc-1-luc cell suspension was prepared at a concentration of about  $2 \times 10^7$  per ml in a 1:1 (v/v) mixture of DMEM and Matrigel. Tumor cells were then injected into the pancreas of male athymic nude mice (6–8 weeks, Charles River) following a surgical procedure [55,56]. Briefly, after mice were anesthetized using isoflurane, the skin and peritoneum were cut open about 1 cm in length using sterile surgical scalpels. The pancreas was pulled out, and about 50  $\mu\text{l}$  of the cell suspension was injected slowly until a small bleb was formed. After the needle was

**Table 1.** Cytotoxic activity of DHA-dFdC against NCI-60 DTP Human Tumor Cell Lines

	Cell line	GI <sub>50</sub> (μM)	TGI (μM)	LC <sub>50</sub> (μM)
Leukemia	CCRF-CEM	0.0507	17.9	>100
	HL-60 (TB)	0.029	14.8	>100
	K-562	0.0674	46.9	>100
	MOLT-4	0.0692	13.3	93.1
	RPMI-8226	0.0538	26.9	>100
	SR	0.0141	28.8	>100
Non-small cell lung cancer	A549/ATCC	0.0326	15.4	43.8
	EKVX	0.852	20.4	52.9
	HOP-62	0.0186	4.47	35.2
	HOP-92	0.771	34.5	>100
	NCI-H226	0.0672	2.75	39.2
	NCI-H23	0.0157	12.7	56.6
	NCI-H322M	1.18	19	46
	NCI-H460	0.0153	11.8	43.3
	NCI-H522	0.028	14.2	54.1
	COLO 205	0.143	14.1	50.7
Colon Cancer	HCC-2998	10.6	26.7	67.5
	HCT-116	0.0311	15.3	44.4
	HCT-15	1.86	25.3	87.5
	HT29	0.0683	17.6	45.1
	KM12	1.05	20.2	51.9
	SW-620	0.0759	23.2	84.4
	SF-268	0.0542	12.9	42.3
	SF-295	0.0791	10.9	37.5
CNS Cancer	SF-539	0.0287	0.538	30.6
	SNB-19	0.0223	12.4	61.9
	SNB-75	0.401	25.1	>100
	U251	0.0305	15.2	43.9
	LOX IMVI	0.0414	1.07	77.9
	MALME-3 M	10.1	22.8	51.6
Melanoma	M14	0.0243	0.21	34.8
	MDA-MB-435	0.311	18.1	43.3
	SK-MEL-2	13.2	29.8	67.6
	SK-MEL-28	10.1	23.3	53.8
	SK-MEL-5	0.29	17.1	42.1
	UACC-257	0.518	22.9	56.1
	UACC-62	0.0494	12.5	43
	IGROV1	3.45	22.5	55.3
	OVCAR-3	11.1	23.5	49.6
	OVCAR-4	14.5	28.8	57.2
Ovarian Cancer	OVCAR-5	0.0821	22.5	63.8
	OVCAR-8	0.0345	11.4	43.2
	NCI-ADR-RES	0.0338	14.8	46.9
	SK-OV-3	0.11	14.2	>100
Renal Cancer	786-0	<0.01	14.2	>100
	A498	0.0855	16.1	51.9
	ACHN	<0.01	10.1	39.4
	CAKI-1	0.0253	11.7	34.3
	RXF 393	0.14	15.1	45.1
	SN12C	0.197	4.49	33.8
	TK-10	11.5	29.4	74.9
	UO-31	0.0835	12	37.9
Prostate Cancer	PC-3	10.7	27	67.8
	DU-145	0.0396	12.5	35.3
Breast Cancer	MCF7	<0.01	13.4	42.3
	MDA-MB-231/ATCC	6.82	22.2	53.5
	HS 578 T	17	45.5	>100
	BT-549	0.0454	16.3	44.2
	T-47D	0.0996	17.6	71.9

Values shown are in μM. GI<sub>50</sub> is the concentration of DHA-dFdC at which tumor cell growth was inhibited by 50%. TGI is the concentration at which tumor cell growth was completely inhibited. LC<sub>50</sub> is the concentration at which 50% of the tumor cells were killed.

withdrawn, a small cotton plug was applied for 10 seconds. The pancreas was returned back, the peritoneum was sutured with Monocryl bioresorbable sutures (Ethicon, Somerville, NJ), and the skin was then closed using surgical clips. Mice were SC injected with buprenorphine (0.1 mg/kg) as a pain killer and were left to heal for 1 week. Tumor progress was monitored using an IVIS Spectrum

imaging system (Caliper, Hopkinton, MA). For IVIS imaging, each mouse was IP injected with a luciferin solution (15 mg/ml) at a dose of 0.15 mg/g body weight in sterile Dulbecco's phosphate buffer saline, anesthetized with isoflurane, and imaged 10 minutes after luciferin injection. Four weeks after tumor implantation, mice with tumors were randomized into 3 groups ( $n = 5-7$ ) and IP injected with DHA-dFdC (50 mg/kg,  $\sim 0.087$  mol/kg) or dFdC (26.1 mg/ml,  $\sim 0.087$  mol/kg), or left untreated. Again, DHA-dFdC was dissolved in a Tween 80/ethanol/water solution with 5% (w/v) of mannitol, and dFdC was dissolved in sterile mannitol solution (5%, w/v). Treatments were repeated twice a week for a total of seven times. Thirty days after the first treatment, mice were sacrificed, and tumors were dissected from the pancreas, weighed, fixed in formalin, dehydrated in 70% ethanol, and embedded in paraffin wax.

In both studies mentioned above, the doses were based on the average weight of mice in the same group on the day of injection and were adjusted only if the weight of an individual mouse was above or below 10% of the average weight.

*Mice with subcutaneous TC-1 tumors.* The *in vivo* antitumor activity of DHA-dFdC was also evaluated in female C57BL/6 mice (6-8 weeks, Charles River) with SC implanted TC-1 mouse lung cancer cells. Briefly,  $5 \times 10^5$  cells in RPMI were SC injected in the right flank of female C57BL/6 mice. Eight days later, mice were randomized into 3 groups ( $n = 5-6$ ) and IP injected with DHA-dFdC (50 mg/kg,  $\sim 0.087$  mol/kg) or dFdC solution (26.1 mg/kg,  $\sim 0.087$  mol/kg), or left untreated as a control. Treatments were repeated every 3 to 4 days for a total of 4 times. Tumor growth was monitored using a digital caliper.

### Immunohistochemistry

Tumor tissues were sectioned and stained in the Histology and Tissue Analysis Core at Dell Pediatric Research Institute at the University of Texas at Austin or in the Department of Molecular Carcinogenesis at the University of Texas M.D. Anderson Cancer Center at Science Park (Smithville, TX) with hematoxylin and eosin (H&E), or antibodies against cleaved lamin-A (apoptosis marker) or Ki-67 (proliferation marker). Slides were then scanned, and images were taken using the ScanScope XT (Aperio Technologies, Vista, CA). In the animal study using Kras Ink4A<sup>+/−</sup> mice, pancreas tissues were examined to evaluate the progression of pancreatic ductal adenocarcinoma (PDAC).

### Statistical Analysis

Statistical analyses were completed by performing analysis of variance followed by Fisher's protected least significant difference procedure. Survival curve comparisons were constructed using Kaplan-Meier survival analysis (GraphPad Prism). The survival curves were compared using the log-rank test (Mantel-Cox test). A *P* value of  $\leq .05$  (two-tailed) was considered statistically significant.

## Results

### Solubility, Partition Coefficient, and Stability of DHA-dFdC

Beall et al. reported a method to measure the aqueous solubility of drug molecules that are unstable in water [46], which was adopted in the present study. To validate the method, the aqueous solubility of 4-(*N*)-stearoyl dFdC, another lipophilic dFdC conjugate [24], which is stable in water, was measured directly (i.e., direct method) or using the indirect method reported by Beall et al. [46]. The solubility of 4-(*N*)-stearoyl dFdC in water was found to be  $1.38 \pm 1.60$  μg/ml when it was measured using the direct method and  $1.39 \pm 0.10$  μg/ml using the indirect method. Therefore, the indirect method was used to

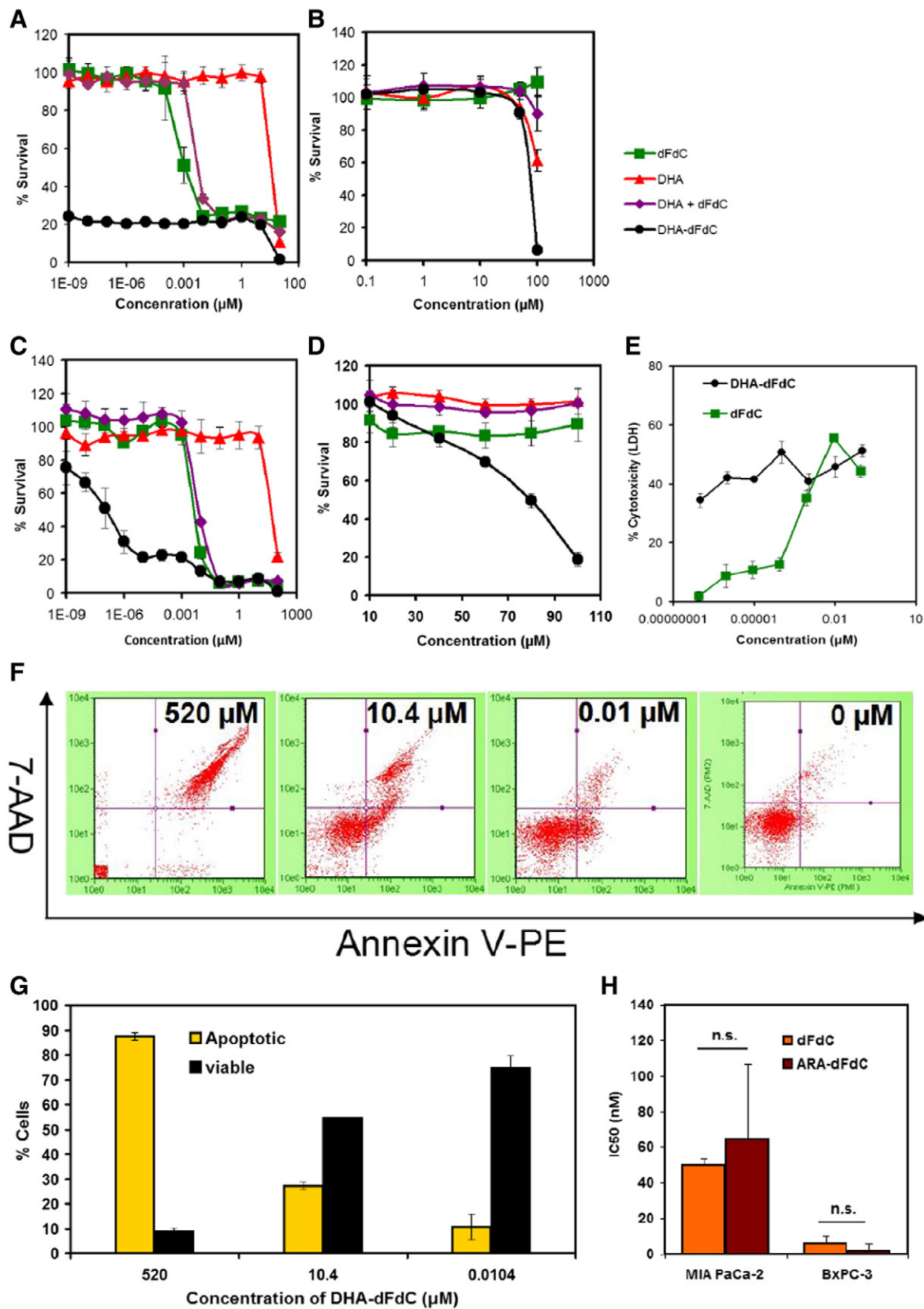


**Figure 3.** (A-D) Cytotoxicity of DHA-dFdC and molar equivalent concentrations of other treatments against BxPC-3 cells after 72 hours (A), Panc-1-luc cells after 24 hours (B), Panc-02 cells after 48 hours (C), and Panc-02 cells after 4 hours (D) of incubation, all measured using an MTT assay. (E) Cytotoxicity of DHA-dFdC and dFdC against Panc-02 cells after 48 hours of incubation, measured using an LDH assay. (F) Proapoptotic activity of DHA-dFdC against Panc-02 cells after staining with Annexin V-PE and 7-AAD. Quarters are: top left, cellular debris, bottom left: live cells, top right: late apoptotic cells, and bottom right: early apoptotic cells. (G) Percent of viable and apoptotic cells after Panc-02 cells were treated with various concentrations of DHA-dFdC. (H) A comparison of the IC<sub>50</sub> values of dFdC and ARA-dFdC in MIA PaCa-2 and BxPC-3 cells (n.s., not significant). Data shown are mean  $\pm$  SD ( $n > 3$ ).



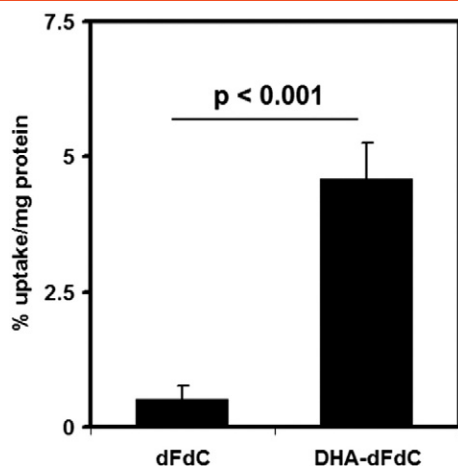


**Figure 4.** Uptake of DHA-dFdC by Panc-02 cells in culture. Cells (250,000/well) were coincubated with DHA-dFdC (10  $\mu$ M in DMSO) or dFdC (10  $\mu$ M in cell culture medium) for 4 hours. Data are mean  $\pm$  SD ( $n = 3-4$ ).

measure the solubility of DHA-dFdC in water, which was found to be  $25.15 \pm 11.20$   $\mu$ g/ml.

The partition coefficient of DHA-dFdC in octanol versus PBS (pH 7.4) was also measured using an indirect method by determining its concentration in octanol before and after partitioning. The log $P$  value of DHA-dFdC was found to be  $2.24 \pm 0.25$ .

DHA-dFdC solubilized in a Tween 80/ethanol/water formulation was found to degrade considerably at room temperature ( $\sim 22^\circ\text{C}$ ) (Figure 1A). The degradation was significantly slower at  $4^\circ\text{C}$  and was also significantly slower in the presence of vitamin E. Vitamin E at 0.01% (w/v) was more effective than at 0.04% (w/v). It was reported previously that a higher concentration of vitamin E may not necessarily have a higher antioxidative activity [57]. The effect of temperature on the chemical stability of DHA-dFdC is shown in Figure 1B. The activation energy of the chemical reaction was calculated to be 12.86 kcal/mol.

#### XRD, UV/Vis, and DSC Profiles of DHA-dFdC

X-ray diffraction pattern showed that the major crystallinity peaks related to dFdC at the 2 theta values of 9.5, 15.4, 19.0, 21.0, 23.0, 27.5, 30.5, and 35.5 were retained in the physical mixture of dFdC and DHA but disappeared in DHA-dFdC (Figure 2A). UV/Vis scanning revealed that the maximum absorption peak ( $\lambda_{\text{max}}$ ) of DHA-dFdC in methanol was 248 nm, and there is another absorption peak at 300 nm (Figure 2B). The  $\lambda_{\text{max}}$  values of dFdC and DHA were 276 nm and 234 nm, respectively (Figure 2B). DSC analysis of DHA-dFdC showed a melting point of  $\sim 96^\circ\text{C}$  (Figure 2C).

#### The Cytotoxicity of DHA-dFdC against Tumor Cells in Culture

The cytotoxicity of DHA-dFdC was evaluated in the NCI-60 DTP human tumor cell lines, and the results are shown in Table 1. In about two thirds of the cell lines tested, DHA-dFdC was more potent than dFdC (Figure S2, Supplement). The NCI-60 DTP human tumor cell lines do not include any pancreatic tumor cell line; therefore, the cytotoxicity of DHA-dFdC was evaluated in several human and mouse pancreatic cancer cell lines (i.e., Panc-02, Bx-PC3, Panc-1) using an MTT assay. In all three cell lines, DHA-dFdC was more cytotoxic than dFdC or the physical mixture of dFdC and DHA

(1:1, molar ratio), and the physical mixture of DHA and dFdC was not more cytotoxic than dFdC alone (Figure 3, A–D). LDH assay also confirmed that DHA-dFdC was more cytotoxic than dFdC in Panc-02 tumor cells (Figure 3E). Data in Figure 3, F and G, show that DHA-dFdC induced tumor cell apoptosis.

To understand the effect of the omega-3 PUFA nature of the DHA (i.e., the docosahexaenoyl group) in the DHA-dFdC on its cytotoxicity against tumor cells, the cytotoxicity of ARA-dFdC, a conjugate of dFdC and ARA, an omega-6 PUFA, was also evaluated in BxPC-3 and MIA PaCa-2 cells, and data in Figure 3H showed that ARA-dFdC was not significantly more cytotoxic than dFdC.

#### Uptake of DHA-dFdC by Tumor Cells in Culture

The percent of DHA-dFdC or dFdC that was taken up by Panc-02 cells after 4 hours of incubation is shown in Figure 4. The uptake of the DHA-dFdC was about 10-fold higher than that of dFdC.

#### Pharmacokinetics and Pancreatic Uptake of DHA-dFdC

The plasma DHA-dFdC levels in mice at different time points after IV injection are shown in Figure 5A. The elimination of DHA-dFdC in mouse plasma appears to follow a biexponential model. Selected pharmacokinetics parameters of DHA-dFdC are shown in Figure 5B. Preliminary study revealed that the concentration of DHA-dFdC in the pancreas of healthy mice 1 hour following IV injection of DHA-dFdC was among the highest compared with DHA-dFdC concentrations in the liver, kidney, spleen, lung, and heart (data not shown). Because monotherapy with dFdC is one of the first-line treatments for advanced pancreatic cancer, the levels of DHA-dFdC in mouse pancreas at various time points after IV injection were also determined and compared with those of dFdC (Figure 5C). The AUC $_{0-\infty}$  values for DHA-dFdC and dFdC were found to be 2408.00  $\mu\text{g/g}\cdot\text{min}$  and 787.71  $\mu\text{g/g}\cdot\text{min}$ , respectively.

#### Antitumor Activity of DHA-dFdC in Mouse Models

Because the cytotoxicity of the DHA-dFdC was up to  $10^5$ -fold higher than that of dFdC in pancreatic tumor cell lines and DHA-dFdC showed relatively higher residence in mouse pancreas compared with dFdC, the antitumor activity of DHA-dFdC was initially tested in Kras Ink4a $^{+/-}$  transgenic mice that spontaneously develop pancreatic tumor. Data in Figure 6A showed that treatment with DHA-dFdC significantly extended the survival of the transgenic mice. To confirm that the Kras Ink4a $^{+/-}$  mice died of pancreatic cancer, mice were euthanized after 10 doses of DHA-dFdC. As shown in Figure 6B, when left untreated, four of six mice showed that the pancreas was replaced with PDAC, whereas the pancreas in the other two mice showed several foci of PDAC and extensive pancreatic intraepithelial neoplasia (PanIN)-2 and PanIN-3. When the mice were treated with DHA-dFdC, the pancreas of only two of six mice was completely replaced by PDAC, and one of six mice had about half of its pancreas replaced with PDAC (Figure 6B). The pancreases in two mice showed variable levels of PanIN-1, -2, and -3, with only limited PDAC foci, and the pancreas of one mouse appeared to be normal (Figure 6B).

The antitumor activity of DHA-dFdC was then evaluated and compared with that of the dFdC or the physical mixture of dFdC and DHA in mice with SC injected human Panc-1-luc tumor cells. As shown in Figure 7A, at the dosing regimen used, DHA-dFdC significantly inhibited Panc-1-luc tumor growth as compared with the vehicle control, but the molar equivalent doses of dFdC alone, DHA

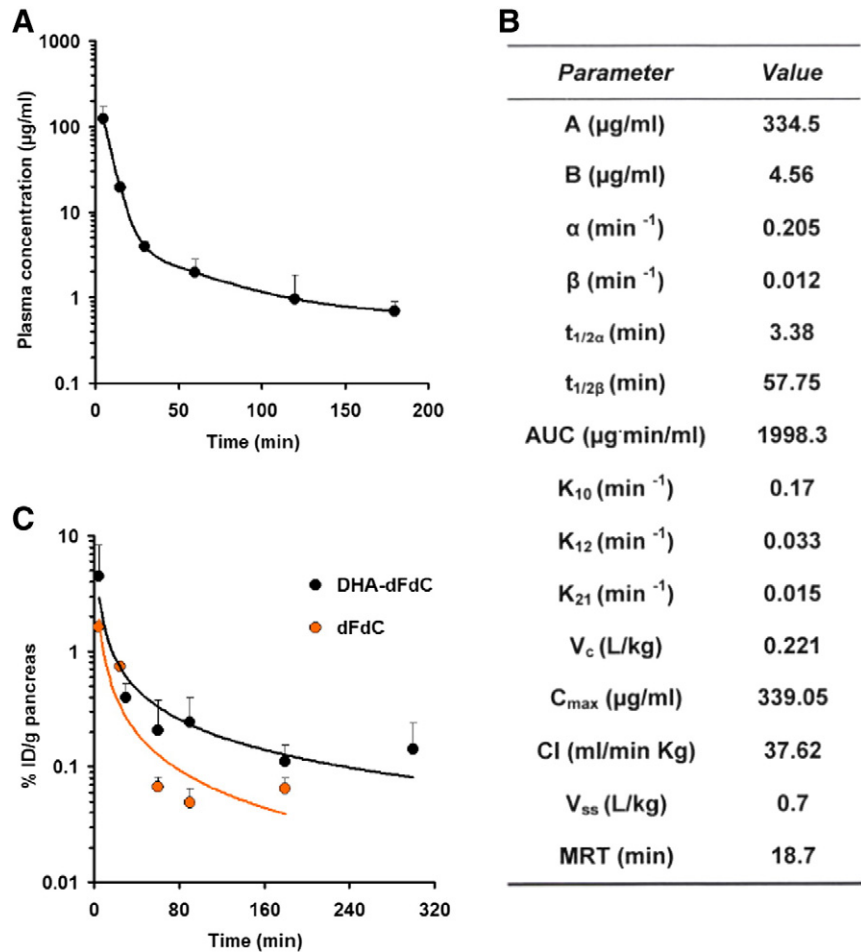


**Figure 5.** Plasma and pancreatic tissue pharmacokinetics of DHA-dFdC. (A) Plasma DHA-dFdC concentration-time curve following IV injection of DHA-dFdC into C57BL/6 mice (75 mg/kg). (B) Selected plasma pharmacokinetics parameters of DHA-dFdC. Data in A were fitted in two-compartment model. (C) Pancreatic tissue DHA-dFdC and dFdC concentration curves following IV injection of BALB/c mice with DHA-dFdC or dFdC alone (75 mg/kg). Data in A and C are mean  $\pm$  SD ( $n = 3-4$ ).

alone, or the physical mixture of dFdC and DHA (1:1 molar ratio) did not significantly inhibit the tumor growth. Shown in Figure 7B are body weights of mice that were treated with DHA-dFdC, DHA alone, dFdC alone, or the physical mixture of DHA and dFdC.

In mice with orthotopic Panc-1-luc tumors, DHA-dFdC at the dosing regimen tested significantly inhibited the tumor growth, but the molar equivalent dFdC did not show significant activity (Figure 8, A–C). Shown in Figure 8D are the body weights of mice that were treated with DHA-dFdC or dFdC. H&E staining of the tumor tissues revealed that tumors in mice that were left untreated have much larger tumor volume and the tumors are poorly differentiated (Figure 9A). In addition, areas of necrosis can be seen in the centers of the tumors (lined in green). A similar pattern was observed in tumors in mice that were treated with dFdC but with less necrosis (Figure 9A). On the contrary, tumors in mice that were treated with DHA-dFdC showed smaller tumor volume (Figure 9A). Ki-67 staining showed that there is a significantly lower cell proliferative index (Ki-67) in tumors in mice that were treated with DHA-dFdC when compared with mice that were treated with dFdC (Figure 9, A and B). Anti-cleaved lamin-A staining showed a significantly higher percent of positive staining in tumors in mice that were treated with DHA-dFdC than in mice that were untreated, whereas the extent of cleaved lamin A–

positive staining in tumors in mice that were treated with dFdC was not different from that in mice that were left untreated (Figure 9, A and C).

Finally, as shown in Figure S3, DHA-dFdC was more effective than the molar equivalent dose of dFdC in inhibiting the growth of SC implanted TC-1 mouse lung cancer cells, demonstrating that the *in vivo* antitumor activity of DHA-dFdC is not limited to pancreatic tumors.

**Discussion**

In the present study, we reported the synthesis of DHA-dFdC, an amide, by conjugating DHA and dFdC and presented <sup>1</sup>H NMR, MS, and LC/MS data to confirm its structure and purity. DHA-dFdC showed potent and broad-spectrum antitumor activity against all of the NCI-60 human tumor cell lines and several human and mouse pancreatic tumor cell lines (Table 1, Figure 3). Unexpectedly, biodistribution studies revealed that DHA-dFdC had a relatively higher accumulation and slower clearance in mouse pancreas after IV injection when compared with dFdC (Figure 5C). Importantly, DHA-dFdC significantly extended the survival of Kras Ink4a<sup>+/-</sup> transgenic mice that spontaneously develop pancreatic tumors and showed a significantly stronger antitumor activity than

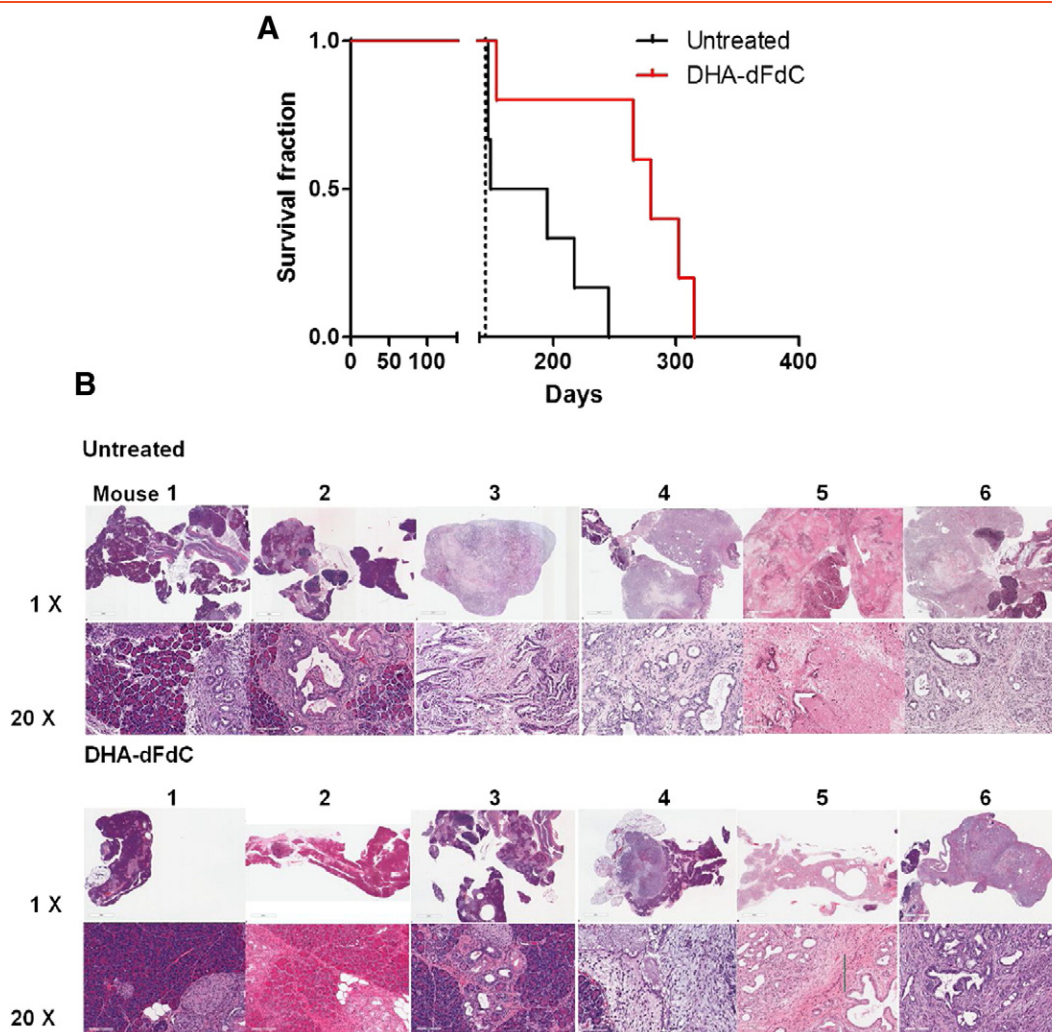


**Figure 6.** Antitumor activity of DHA-dFdC in *Kras Ink4a*<sup>+/-</sup> mice. (A) Survival curves of female *Kras Ink4a*<sup>+/-</sup> mice treated with DHA-dFdC or left untreated. Mice were shifted from normal diet to a high-fat diet at 16 weeks of age. DHA-dFdC treatment (50 mg/kg, IP twice a week) was started when mice were at the age of 20 weeks. (B) Representative H&E images of mouse pancreas and pancreatic tumors from *Kras Ink4a*<sup>+/-</sup> transgenic mice that were treated with DHA-dFdC (IP 65 mg/kg, up to twice a week) or left untreated (*n* = 6). Each tissue is represented by two magnifications: top: 1 × and bottom: 20 ×. The scale bar in each 1 × image represents 2 mm, and that in each 20 × image represents 100 μm.

the molar equivalent dose of dFdC in mouse models with subcutaneous and orthotopic Panc-1 human pancreatic tumors (Figures 7-9).

There have been numerous previously reported dFdC derivatives [33,37,39,41,58-65], including our own [25], but in many cases, the derivatives were not more cytotoxic than dFdC alone against tumor cells in culture [59,60,64]. Similarly, the chemical conjugates of DHA and other cancer chemotherapeutic agents such as paclitaxel, doxorubicin, and 10-hydroxycamptothecin were previously reported as well, but the conjugates were not more cytotoxic than the original agents in cell culture [12-14]. In fact, these conjugates were considered prodrugs that need to be converted to active forms to be effective [12,14]. Therefore, it was unexpected that DHA-dFdC showed a potent broad-spectrum antitumor activity and was significantly more cytotoxic than dFdC in pancreatic cancer cells (e.g., in BxPC-3 cells, the IC<sub>50</sub> value of DHA-dFdC was more than 100,000 fold smaller than that of the dFdC) and many of the NCI-60 DTP human tumor cell lines (Figure S2).

DHA-dFdC induced tumor cells to undergo apoptosis (e.g., Panc-02 in Figure 3F), and it is expected that the dFdC formed following the hydrolysis of DHA-dFdC contributed to the apoptosis. However, the mechanism underlying the potent antitumor activity of DHA-dFdC appears to be different from that of dFdC alone and may not even be primarily attributed to dFdC's activity in inhibiting nucleic acid synthesis [66-68]. For example, although the conjugation of DHA to the 4-NH<sub>2</sub> group on the dFdC is expected to prevent its deamination, the mere protection of the 4-NH<sub>2</sub> is not sufficient to increase the antitumor activity of dFdC, as the 4-(*N*)-stearoyl dFdC, a conjugate of dFdC with stearate in the 4-NH<sub>2</sub> position, was not significantly more cytotoxic than dFdC against various dFdC-sensitive cancer cell lines [23,31,69]. Therefore, it is unlikely that the potent antitumor activity of the DHA-dFdC was simply due to the protection of the vulnerable amine group on the dFdC. Instead, it appears that the omega-3 PUFA nature of the docosahexaenoyl group in the DHA-dFdC is critical for its strong antitumor activity. ARA is a



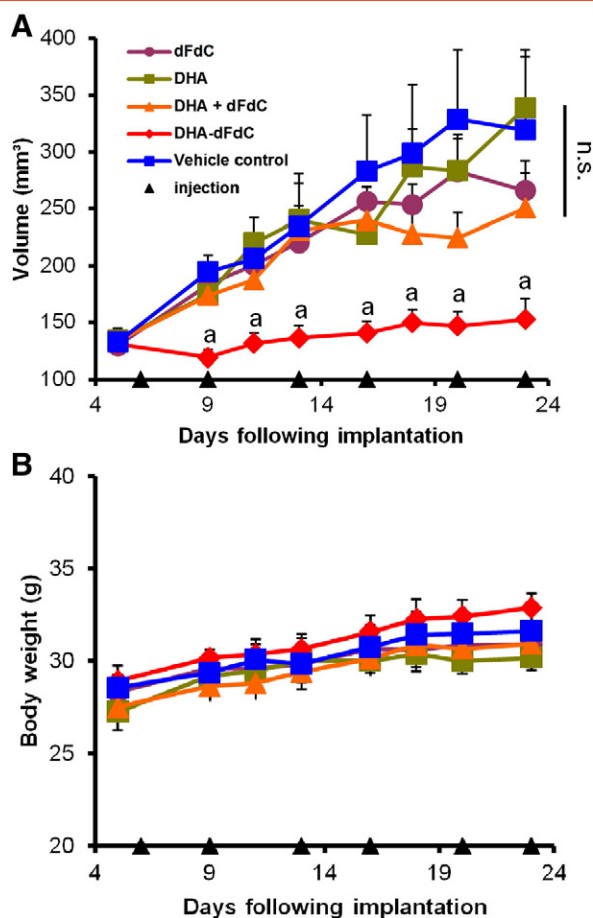


**Figure 7.** Antitumor activity of DHA-dFdC against Panc-1-luc human pancreatic tumors implanted SC in nude male mice. Tumor cells ( $5 \times 10^6$  cells/mouse) were injected (SC) in the right flank of mice on day 0. On day 5, mice were randomized and treated with DHA-dFdC (50 mg/kg) or molar equivalents of DHA, dFdC, or DHA + dFdC. Control mice were injected with an aqueous solution of Tween 80/ethanol in 5% of mannitol as a vehicle control. All treatments were given by IP injection twice a week. (A) Tumor growth curves. (B) Mouse body weights. Data are mean  $\pm$  SD ( $n = 5-6$ ). (<sup>a</sup> $P < .05$ , DHA-dFdC versus other groups; n.s., not significant).

PUFA as well, but it is an omega-6 PUFA, and ARA-dFdC was not more cytotoxic than dFdC in the cell lines tested (Figure 3H). It was reported previously that epoxy derivatives of DHA, formed by the action of cytochrome p450 epoxigenases, exhibited antiproliferative, antiangiogenic, and antimetastatic activity [70]. It is expected that DHA-dFdC may also undergo oxidation at the 4 to 5, 7 to 8, 10 to 11, 13 to 14, 16 to 17, or 19 to 20 sites on its docosahexaenoyl moiety to form the epoxy derivatives, and the oxidized metabolites of DHA-dFdC may have antitumor activity as well. The potent *in vitro* cytotoxicity of the DHA-dFdC may also be related to the more extensive and/or faster cellular uptake of the DHA-dFdC by tumor cells in culture than the uptake of the dFdC alone (Figure 4) but may not be entirely attributed to the increased cellular uptake. For example, when Panc-02 cells were treated with DHA-dFdC or dFdC at high concentrations (e.g., 10-100  $\mu$ M), cytotoxicity was detected after only 4 hours of incubation with DHA-dFdC but not with dFdC (Figure 3D). The dFdC, which inhibits nucleic acid synthesis

and thus cell proliferation, showed significant activity only after prolonged incubation (Figure 3C). Therefore, it is possible that DHA-dFdC, at least at high concentrations, may cause tumor cell death in a cell cycle-independent manner, and the cell death is unlikely to be simply due to the DHA moiety in the DHA-dFdC because DHA alone at the same concentrations did not show significant cytotoxicity after 4 hours of incubation (Figure 3D). Taken together, it appears that the mechanisms underlying the cytotoxicity of the DHA-dFdC and dFdC alone are not identical, but more experiments need to be carried out to understand how DHA-dFdC causes cytotoxicity to tumor cells.

Another unexpected finding is the relatively longer residence time of DHA-dFdC in pancreas after IV injection into mice as compared with dFdC (Figure 5C). Although a high concentration of DHA-dFdC in the pancreas does not necessarily indicate that the content of DHA-dFdC in mouse pancreatic tumor tissues was also high, one can expect the longer residence time of DHA-dFdC in pancreas to increase the exposure of pancreatic tumor cells to DHA-dFdC. The high accumulation of DHA-dFdC in the pancreas is likely related to the slow elimination of the DHA-dFdC from pancreatic tissues (Figure 5D), but the exact reason behind the relatively slow pancreatic elimination remains unknown. Fukui et al. previously reported that when a diet supplemented with fish oil was given to nude mice for 2 weeks (orally), a relatively high level of eicosapentanoic acid (another omega-3 fatty acid) was detected in the pancreas of the mice compared with control mice that received diet supplemented with corn oil [71]. Significantly higher pancreatic accumulation of DHA was also reported by Fukui and coworkers when compared with control mice [71], but the difference in DHA levels between fish oil-fed and corn oil-fed mice was much less pronounced than that reported with eicosapentanoic acid (about 1.5-fold vs. 5-fold) [71]. Li et al. also reported the synthesis of a DHA and dFdC conjugate, although data were not presented to demonstrate that the DHA was conjugated to the 4-NH<sub>2</sub> group of dFdC [72]. Nonetheless, the authors showed that DHA seemed to help target compounds conjugated to it into cells whose membrane is rich in phosphatidylethanolamine [72].

The unexpected higher accumulation of DHA-dFdC in pancreas (relative to dFdC), in addition to its strong cytotoxicity in several pancreatic tumor cell lines, prompted the evaluation of its antitumor activity against pancreatic tumors in mouse models, and data in Figures 6 to 9 clearly showed that DHA-dFdC, at a dosing regimen that did not cause any observed side effects, effectively inhibited pancreatic tumor growth in mice with spontaneously developed PDAC and with subcutaneous or orthotopic Panc-1-luc human pancreatic tumor xenografts. Panc-1 tumor cells are known to be resistant to dFdC [73], which explains why dFdC at the dosing regimen used did not significantly inhibit Panc-1-luc tumor growth (Figures 8–9). The potent cytotoxicity of DHA-dFdC against pancreatic tumor cells and their longer residence time in pancreas may partially explain its observed potent antitumor activity against orthotopic Panc-1 tumors in nude mice and pancreatic tumors spontaneously developed in the Kras ink4a<sup>+/−</sup> transgenic mice. In addition, data from the NCI-60 human tumor cell line screening clearly showed that DHA-dFdC has potent broad-spectrum activity against many tumor cells. Thus, it is not unreasonable to expect it to show potent antitumor activity against other tumors such as renal cell carcinoma and leukemia. In fact, DHA-dFdC was significantly more effective than the molar equivalent dose of dFdC



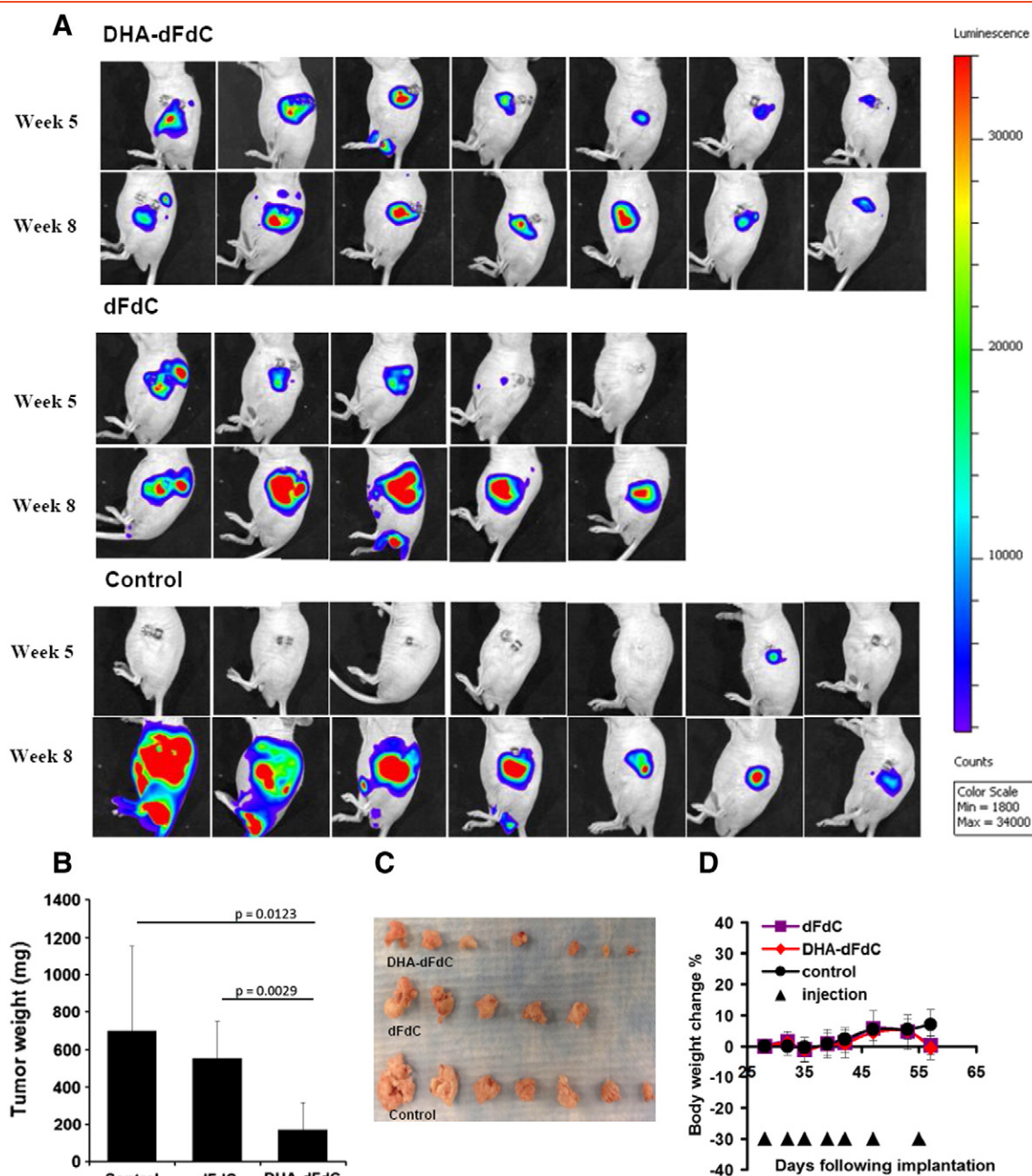


**Figure 8.** Antitumor activity of DHA-dFdC against orthotopic Panc-1-luc pancreatic tumors in nude male mice. Panc-1-luc cells ( $1 \times 10^6$  cells/mouse) were injected in mouse pancreas. Four weeks later, mice were randomized and treated with DHA-dFdC (50 mg/kg) or dFdC (26.1 mg/kg) (IP injection twice a week). (A) IVIS images of tumors in the fifth week and eighth week after the tumor implantation. (B) Tumor weights at the end of the study. (C) A digital photograph of tumors at the end of the study. (D) Mouse body weight change during treatments. Data shown in B and D are means  $\pm$  SD ( $n = 5-7$ ).

in inhibiting the growth of SC implanted mouse TC-1 lung cancer cells (Figure S3). In summary, data in the present study clearly demonstrated that covalently conjugating two pharmacologically active compounds together can generate a new compound with unexpected pharmacokinetics and efficacy profiles.

## Conclusion

A novel amide (DHA-dFdC) was synthesized by conjugating DHA, an omega-3 PUFA, with dFdC, a nucleoside analogue. DHA-dFdC

showed potent and broad-spectrum antitumor activity in cell culture and high distribution in mouse pancreas after IV injection. Importantly, DHA-dFdC effectively inhibited tumor growth in transgenic mice that spontaneously develop pancreatic tumor and in nude mice with orthotopic pancreatic tumor.

## Appendix A. Supplementary data

Supplementary data to this article can be found online at <http://dx.doi.org/10.1016/j.neo.2015.11.012>.

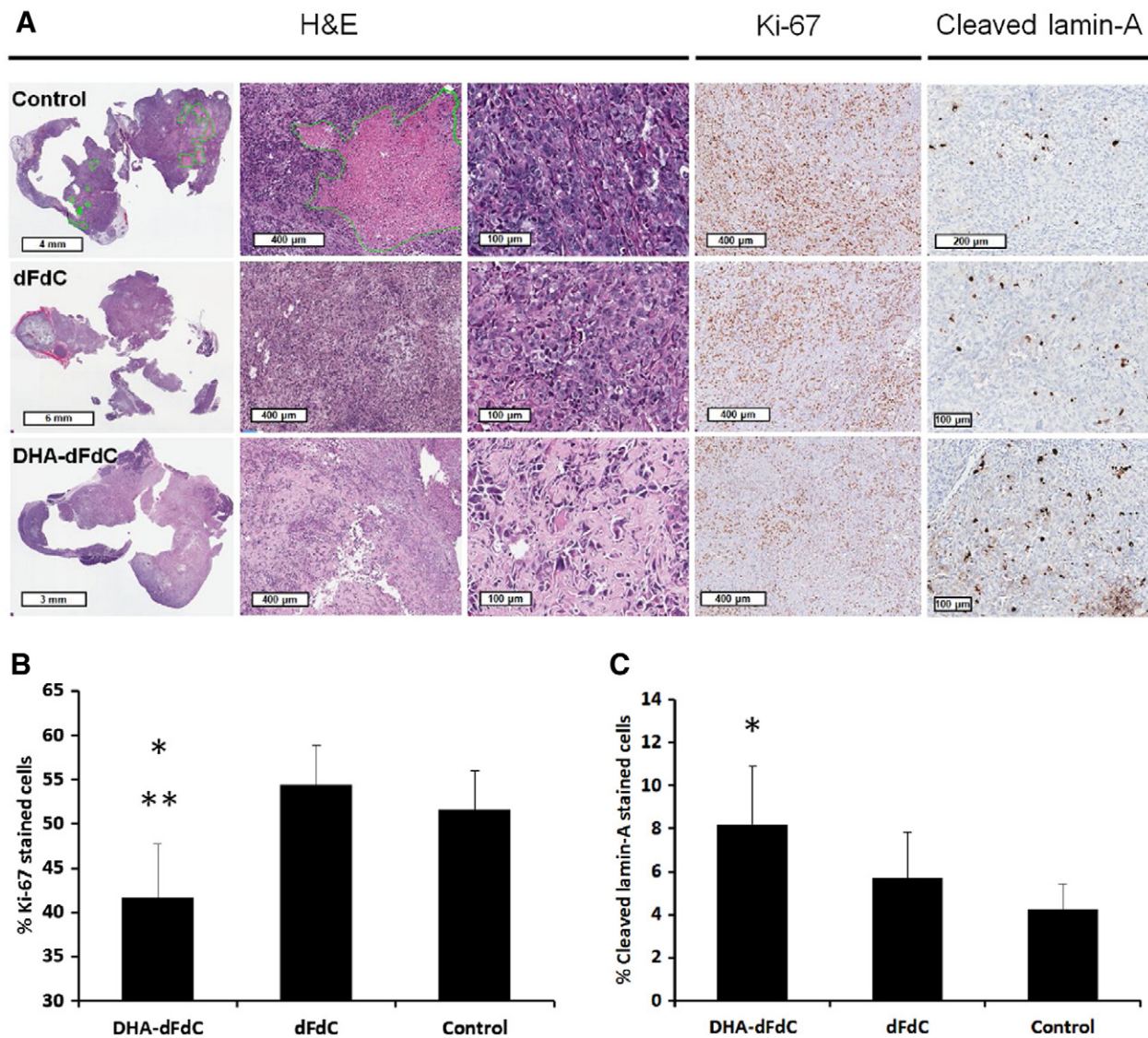


**Figure 9.** (A) Representative histological images of tumors from nude mice that were treated with DHA-dFdC or dFdC after the tumor tissues were stained with H&E, anti-Ki-67, or anti-cleaved lamin-A antibodies. The areas outlined in green (in the H&E staining images) represent necrosis. (B) Percentage of Ki-67 positively stained cells. (C) Percent of cleaved lamin A positively stained cells. \* $P < .05$  against control, \*\* $P < .05$  against dFdC.

## References

- [1] Murphy RA, Mourtzakis M, Chu QS, Baracos VE, Reiman T, and Mazurak VC (2011). Supplementation with fish oil increases first-line chemotherapy efficacy in patients with advanced nonsmall cell lung cancer. *Cancer* **117**, 3774–3780.
- [2] Arshad A, Chung WY, Steward W, Metcalfe MS, and Dennison AR (2013). Reduction in circulating pro-angiogenic and pro-inflammatory factors is related to improved outcomes in patients with advanced pancreatic cancer treated with gemcitabine and intravenous omega-3 fish oil. *HPB (Oxford)* **15**, 428–432.
- [3] Wynter MP, Russell ST, and Tisdale MJ (2004). Effect of n-3 fatty acids on the antitumour effects of cytotoxic drugs. *In Vivo* **18**, 543–547.
- [4] Kato T, Kolenic N, and Pardini RS (2007). Docosahexaenoic acid (DHA), a primary tumor suppressive omega-3 fatty acid, inhibits growth of colorectal cancer independent of p53 mutational status. *Nutr Cancer* **58**, 178–187.
- [5] Strouch MJ, Ding Y, Salabat MR, Melstrom LG, Adrian K, Quinn C, Pelham C, Rao S, Adrian TE, and Bentrem DJ, et al (2011). A high omega-3 fatty acid diet mitigates murine pancreatic precancer development. *J Surg Res* **165**, 75–81.
- [6] Merendino N, Loppi B, D'Aquino M, Molinari R, Pessina G, Romano C, and Velotti F (2005). Docosahexaenoic acid induces apoptosis in the human PaCa-44 pancreatic cancer cell line by active reduced glutathione extrusion and lipid peroxidation. *Nutr Cancer* **52**, 225–233.
- [7] Merendino N, Molinari R, Loppi B, Pessina G, D'Aquino M, Tomassi G, and Velotti F (2003). Induction of apoptosis in human pancreatic cancer cells by docosahexaenoic acid. *Ann N Y Acad Sci* **1010**, 361–364.
- [8] D'Eliseo D, Manzi L, Merendino N, and Velotti F (2012). Docosahexaenoic acid inhibits invasion of human RT112 urinary bladder and PT45 pancreatic carcinoma cells via down-modulation of granzyme B expression. *J Nutr Biochem* **23**, 452–457.
- [9] Chen HW, Chao CY, Lin LL, Lu CY, Liu KL, Lii CK, and Li CC (2013). Inhibition of matrix metalloproteinase-9 expression by docosahexaenoic acid mediated by heme oxygenase 1 in 12-O-tetradecanoylphorbol-13-acetate-induced MCF-7 human breast cancer cells. *Arch Toxicol* **87**, 857–869.
- [10] Rahman MM, Veigas JM, Williams PJ, and Fernandes G (2013). DHA is a more potent inhibitor of breast cancer metastasis to bone and related osteolysis than EPA. *Breast Cancer Res Treat* **141**, 341–352.
- [11] Spencer L, Mann C, Metcalfe M, Webb M, Pollard C, Spencer D, Berry D, Steward W, and Dennison A (2009). The effect of omega-3 FAs on tumour angiogenesis and their therapeutic potential. *Eur J Cancer* **45**, 2077–2086.
- [12] Wang Y, Li L, Jiang W, Yang Z, and Zhang Z (2006). Synthesis and preliminary antitumor activity evaluation of a DHA and doxorubicin conjugate. *Bioorg Med Chem Lett* **16**, 2974–2977.
- [13] Wang Y, Li L, Jiang W, and Larrick JW (2005). Synthesis and evaluation of a DHA and 10-hydroxycamptothecin conjugate. *Bioorg Med Chem* **13**, 5592–5599.



- [14] Bradley MO, Webb NL, Anthony FH, Devanesan P, Witman PA, Hemamalini S, Chander MC, Baker SD, He L, and Horwitz SB, et al (2001). Tumor targeting by covalent conjugation of a natural fatty acid to paclitaxel. *Clin Cancer Res* 7, 3229–3238.
- [15] Bedikian AY, DeConti RC, Conry R, Agarwala S, Papadopoulos N, Kim KB, and Ernstoff M (2011). Phase 3 study of docosahexaenoic acid-paclitaxel versus dacarbazine in patients with metastatic malignant melanoma. *Ann Oncol* 22, 787–793.
- [16] Homs J, Bedikian AY, Papadopoulos NE, Kim KB, Hwu WJ, Mahoney SL, and Hwu P (2010). Phase 2 open-label study of weekly docosahexaenoic acid-paclitaxel in patients with metastatic uveal melanoma. *Melanoma Res* 20, 507–510.
- [17] Sparreboom A, Wolff AC, Verweij J, Zabelina Y, van Zomeren DM, McIntire GL, Swindell CS, Donehower RC, and Baker SD (2003). Disposition of docosahexaenoic acid-paclitaxel, a novel taxane, in blood: in vitro and clinical pharmacokinetic studies. *Clin Cancer Res* 9, 151–159.
- [18] Bradley MO, Swindell CS, Anthony FH, Witman PA, Devanesan P, Webb NL, Baker SD, Wolff AC, and Donehower RC (2001). Tumor targeting by conjugation of DHA to paclitaxel. *J Control Release* 74, 233–236.
- [19] Hui YF and Reitz J (1997). Gemcitabine: a cytidine analogue active against solid tumors. *Am J Health Syst Pharm* 54, 162–170.
- [20] Pierantoni C, Pagliacci A, Scartozzi M, Berardi R, Bianconi M, and Cascinu S (2008). Pancreatic cancer: progress in cancer therapy. *Crit Rev Oncol Hematol* 67, 27–38.
- [21] Kontopodis E, Kentepozidis N, Christophyllakis C, Boukovinas I, Kalykaki A, Kalbakis K, Vamvakas L, Agelaki S, Kotsakis A, and Vardakis N, et al (2015). Docetaxel, gemcitabine and bevacizumab as salvage chemotherapy for HER-2-negative metastatic breast cancer. *Cancer Chemother Pharmacol* 75, 153–160.
- [22] Nadal R and Bellmunt J (2014). New treatments for bladder cancer: when will we make progress? *Curr Treat Options Oncol* 15, 99–114.
- [23] Chung WG, Sandoval MA, Sloat BR, Lansakara P, and Cui Z (2012). Stearoyl gemcitabine nanoparticles overcome resistance related to the overexpression of ribonucleotide reductase subunit M1. *J Control Release* 157, 132–140.
- [24] Sloat BR, Sandoval MA, Li D, Chung WG, Lansakara P, Proteau PJ, Kiguchi K, Digiovanni J, and Cui Z (2011). In vitro and in vivo anti-tumor activities of a gemcitabine derivative carried by nanoparticles. *Int J Pharm* 409, 278–288.
- [25] Lansakara P, Rodriguez BL, and Cui Z (2012). Synthesis and in vitro evaluation of novel lipophilic monophosphorylated gemcitabine derivatives and their nanoparticles. *Int J Pharm* 429, 123–134.
- [26] Moysan E, Bastiat G, and Benoit JP (2013). Gemcitabine versus Modified Gemcitabine: a review of several promising chemical modifications. *Mol Pharm* 10, 430–444.
- [27] Abbruzzese JL, Grunewald R, Weeks EA, Gravel D, Adams T, Nowak B, Mineishi S, Tarassoff P, Satterlee W, and Raber MN, et al (1991). A phase I clinical, plasma, and cellular pharmacology study of gemcitabine. *J Clin Oncol* 9, 491–498.
- [28] Immordino ML, Brusa P, Rocco F, Arpicco S, Ceruti M, and Cattel L (2004). Preparation, characterization, cytotoxicity and pharmacokinetics of liposomes containing lipophilic gemcitabine prodrugs. *J Control Release* 100, 331–346.
- [29] Zhu S, Lansakara P, Li X, and Cui Z (2012). Lysosomal delivery of a lipophilic gemcitabine prodrug using novel acid-sensitive micelles improved its antitumor activity. *Bioconjug Chem* 23, 966–980.
- [30] Sandoval MA, Sloat BR, Lansakara P, Kumar A, Rodriguez BL, Kiguchi K, Digiovanni J, and Cui Z (2012). EGFR-targeted stearoyl gemcitabine nanoparticles show enhanced anti-tumor activity. *J Control Release* 157, 287–296.
- [31] Wonganan P, Lansakara P, Zhu S, Holzer M, Sandoval MA, Warthaka M, and Cui Z (2013). Just getting into cells is not enough: mechanisms underlying 4-(N)-stearoyl gemcitabine solid lipid nanoparticle's ability to overcome gemcitabine resistance caused by RRM1 overexpression. *J Control Release* 169, 17–27.
- [32] De Angel RE, Blando JM, Hogan MG, Sandoval MA, Lansakara P, Dunlap SM, Hursting SD, and Cui Z (2013). Stearoyl gemcitabine nanoparticles overcome obesity-induced cancer cell resistance to gemcitabine in a mouse postmenopausal breast cancer model. *Cancer Biol Ther* 14, 357–364.
- [33] Couvreur P, Stella B, Reddy L H, Hillaireau H, Dubernet C, Desmaele D, Lepetre-Mouelhi S, Rocco F, reudde-Bosquet N, and Clayette P, et al (2006). Squalenoyl nanomedicines as potential therapeutics. *Nano Lett* 6, 2544–2548.
- [34] Tao XM, Wang JC, Wang JB, Feng Q, Gao SY, Zhang LR, and Zhang Q (2012). Enhanced anticancer activity of gemcitabine coupling with conjugated linoleic acid against human breast cancer in vitro and in vivo. *Eur J Pharm Biopharm* 82, 401–409.
- [35] Maksimenko A, Alami M, Zouhiri F, Brion JD, Pruvost A, Mouglin J, Hamze A, Boissenot T, Provot O, and Desmaele D, et al (2014). Therapeutic modalities of squalenoyl nanocomposites in colon cancer: an ongoing search for improved efficacy. *ACS Nano* 8, 2018–2032.
- [36] Arias JL, Reddy LH, Othman M, Gillet B, Desmaele D, Zouhiri F, Dosio F, Gref R, and Couvreur P (2011). Squalene based nanocomposites: a new platform for the design of multifunctional pharmaceutical theragnostics. *ACS Nano* 5, 1513–1521.
- [37] Reddy LH, Renoir JM, Marsaud V, Lepetre-Mouelhi S, Desmaele D, and Couvreur P (2009). Anticancer efficacy of squalenoyl gemcitabine nanomedicine on 60 human tumor cell panel and on experimental tumor. *Mol Pharm* 6, 1526–1535.
- [38] Reddy LH, Ferreira H, Dubernet C, Mouelhi SL, Desmaele D, Rousseau B, and Couvreur P (2008). Squalenoyl nanomedicine of gemcitabine is more potent after oral administration in leukemia-bearing rats: study of mechanisms. *Anticancer Drugs* 19, 999–1006.
- [39] Reddy LH, Marque PE, Dubernet C, Mouelhi SL, Desmaele D, and Couvreur P (2008). Preclinical toxicology (subacute and acute) and efficacy of a new squalenoyl gemcitabine anticancer nanomedicine. *J Pharmacol Exp Ther* 325, 484–490.
- [40] Reddy LH, Dubernet C, Mouelhi SL, Marque PE, Desmaele D, and Couvreur P (2007). A new nanomedicine of gemcitabine displays enhanced anticancer activity in sensitive and resistant leukemia types. *J Control Release* 124, 20–27.
- [41] Rejiba S, Reddy LH, Bigand C, Parmentier C, Couvreur P, and Hajri A (2011). Squalenoyl gemcitabine nanomedicine overcomes the low efficacy of gemcitabine therapy in pancreatic cancer. *Nanomedicine* 7, 841–849.
- [42] Wolfgang CL, Herman JM, Laheru DA, Klein AP, Erdek MA, Fishman EK, and Hruban RH (2013). Recent progress in pancreatic cancer. *CA Cancer J Clin* 63, 318–348.
- [43] Ryan DP, Hong TS, and Bardeesy N (2014). Pancreatic adenocarcinoma. *N Engl J Med* 371, 1039–1049.
- [44] Muniz VP, Barnes JM, Paliwal S, Zhang X, Tang X, Chen S, Zamba KD, Cullen JJ, Meyerholz DK, and Meyers S, et al (2011). The ARF tumor suppressor inhibits tumor cell colonization independent of p53 in a novel mouse model of pancreatic ductal adenocarcinoma metastasis. *Mol Cancer Res* 9, 867–877.
- [45] Guo ZZ and Gallo JM (1999). Selective Protection of 2',2'-Difluorodeoxycytidine (Gemcitabine). *J Org Chem* 64, 8319–8322.
- [46] Beall HD, Getz JJ, and Sloan KB (1993). The estimation of relative water solubility for prodrugs that are unstable in water. *Int J Pharm* 93, 37–47.
- [47] Hsu CH, Jay M, Bummer PM, and Lehmler HJ (2003). Chemical stability of esters of nicotinic acid intended for pulmonary administration by liquid ventilation. *Pharm Res* 20, 918–925.
- [48] Yang J, Kerwin SM, Bowman PD, and Stavchansky S (2012). Stability of caffeic acid phenethyl amide (CAPA) in rat plasma. *Biomed Chromatogr* 26, 594–598.
- [49] Naguib YW, Rodriguez BL, Li X, Hursting SD, Williams III RO, and Cui Z (2014). Solid lipid nanoparticle formulations of docetaxel prepared with high melting point triglycerides: in vitro and in vivo evaluation. *Mol Pharm* 11, 1239–1249.
- [50] Zhu S, Wonganan P, Lansakara P, O'Mary HL, Li Y, and Cui Z (2013). The effect of the acid-sensitivity of 4-(N)-stearoyl gemcitabine-loaded micelles on drug resistance caused by RRM1 overexpression. *Biomaterials* 34, 2327–2339.
- [51] Lanz C, Fruh M, Thormann W, Cerny T, and Lauterburg BH (2007). Rapid determination of gemcitabine in plasma and serum using reversed-phase HPLC. *J Sep Sci* 30, 1811–1820.
- [52] Zhang Y, Huo M, Zhou J, and Xie S (2010). PKSolver: An add-in program for pharmacokinetic and pharmacodynamic data analysis in Microsoft Excel. *Comput Methods Programs Biomed* 99, 306–314.
- [53] Lashinger LM, Harrison LM, Rasmussen AJ, Logsdon CD, Fischer SM, McArthur MJ, and Hursting SD (2013). Dietary energy balance modulation of Kras- and Ink4a/Arf+/-driven pancreatic cancer: the role of insulin-like growth factor-I. *Cancer Prev Res (Phila)* 6, 1046–1055.
- [54] Xu P, Meng Q, Sun H, Yin Q, Yu H, Zhang Z, Cao M, Zhang Y, and Li Y (2015). Shrapnel nanoparticles loading docetaxel inhibit metastasis and growth of breast cancer1. *Biomaterials* 64, 10–20.
- [55] Raut CP, Nawrocki S, Lashinger LM, Davis DW, Khanbolooki S, Xiong H, Ellis LM, and McConkey DJ (2004). Celecoxib inhibits angiogenesis by inducing

- endothelial cell apoptosis in human pancreatic tumor xenografts. *Cancer Biol Ther* **3**, 1217–1224.
- [56] Bruns CJ, Harbison MT, Kuniyasu H, Eue I, and Fidler IJ (1999). In vivo selection and characterization of metastatic variants from human pancreatic adenocarcinoma by using orthotopic implantation in nude mice. *Neoplasia* **1**, 50–62.
- [57] Owen SC (2006). Alpha tocopherol. In: Rowe RC, Sheskey PJ, Owen SC, editors. *Handbook of Pharmaceutical Excipients*. London: Pharmaceutical Press; 2006. p. 32–35.
- [58] Vandana M and Sahoo SK (2010). Long circulation and cytotoxicity of PEGylated gemcitabine and its potential for the treatment of pancreatic cancer. *Biomaterials* **31**, 9340–9356.
- [59] Pasut G, Canal F, Dalla VL, Arpicco S, Veronese FM, and Schiavon O (2008). Antitumoral activity of PEG-gemcitabine prodrugs targeted by folic acid. *J Control Release* **127**, 239–248.
- [60] Guo P, Ma J, Li S, Guo Z, Adams AL, and Gallo JM (2001). Targeted delivery of a peripheral benzodiazepine receptor ligand-gemcitabine conjugate to brain tumors in a xenograft model. *Cancer Chemother Pharmacol* **48**, 169–176.
- [61] Maiti S, Park N, Han JH, Jeon HM, Lee JH, Bhuniya S, Kang C, and Kim JS (2013). Gemcitabine-coumarin-biotin conjugates: a target specific theranostic anticancer prodrug. *J Am Chem Soc* **135**, 4567–4572.
- [62] Ali SM, Khan AR, Ahmad MU, Chen P, Sheikh S, and Ahmad I (2005). Synthesis and biological evaluation of gemcitabine-lipid conjugate (NEO6002). *Bioorg Med Chem Lett* **15**, 2571–2574.
- [63] Alexander RL, Greene BT, Torti SV, and Kucera GL (2005). A novel phospholipid gemcitabine conjugate is able to bypass three drug-resistance mechanisms. *Cancer Chemother Pharmacol* **56**, 15–21.
- [64] Chitkara D, Mittal A, Behrman SW, Kumar N, and Mahato RI (2013). Self-assembling, amphiphilic polymer-gemcitabine conjugate shows enhanced antitumor efficacy against human pancreatic adenocarcinoma. *Bioconjug Chem* **24**, 1161–1173.
- [65] Khare V, Kour S, Alam N, Dubey RD, Saneja A, Koul M, Gupta AP, Singh D, Singh SK, and Saxena AK, et al (2014). Synthesis, characterization and mechanistic-insight into the anti-proliferative potential of PLGA-gemcitabine conjugate. *Int J Pharm* **470**, 51–62.
- [66] Bergman AM, Pinedo HM, and Peters GJ (2002). Determinants of resistance to 2',2'-difluorodeoxycytidine (gemcitabine). *Drug Resist Updat* **5**, 19–33.
- [67] de Sousa CL and Monteiro G (2014). Gemcitabine: metabolism and molecular mechanisms of action, sensitivity and chemoresistance in pancreatic cancer. *Eur J Pharmacol* **741**, 8–16.
- [68] Andersson R, Aho U, Nilsson BI, Peters GJ, Pastor-Anglada M, Rasch W, and Sandvold ML (2009). Gemcitabine chemoresistance in pancreatic cancer: molecular mechanisms and potential solutions. *Scand J Gastroenterol* **44**, 782–786.
- [69] Wang Y, Fan W, Dai X, Katragadda U, Mckinley D, Teng Q, and Tan C (2014). Enhanced tumor delivery of gemcitabine via PEG-DSPE/TPGS mixed micelles. *Mol Pharm* **11**, 1140–1150.
- [70] Zhang G, Panigrahy D, Mahakian LM, Yang J, Liu JY, Stephen Lee KS, Wettersten HI, Ulu A, Hu X, and Tam S, et al (2013). Epoxy metabolites of docosahexaenoic acid (DHA) inhibit angiogenesis, tumor growth, and metastasis. *Proc Natl Acad Sci U S A* **110**, 6530–6535.
- [71] Fukui M, Kang KS, Okada K, and Zhu BT (2013). EPA, an omega-3 fatty acid, induces apoptosis in human pancreatic cancer cells: role of ROS accumulation, caspase-8 activation, and autophagy induction. *J Cell Biochem* **114**, 192–203.
- [72] Li S, Qin J, Tian C, Cao J, Fida G, Wang Z, Chen H, Qian Z, Chen WR, and Gu Y (2014). The targeting mechanism of DHA ligand and its conjugate with Gemcitabine for the enhanced tumor therapy. *Oncotarget* **5**, 3622–3635.
- [73] Duxbury MS, Ito H, Zinner MJ, Ashley SW, and Whang EE (2004). RNA interference targeting the M2 subunit of ribonucleotide reductase enhances pancreatic adenocarcinoma chemosensitivity to gemcitabine. *Oncogene* **23**, 1539–1548.



## Supplemental materials:

### Synthesis, characterization, and *in vitro* and *in vivo* evaluations of 4-(*N*)-docosaheptaenoyl 2', 2'-difluorodeoxycytidine with potent and broad spectrum antitumor activity

Youssef W. Naguib, Dharmika Lansakara-P., Laura M. Lashinger, B. Leticia Rodriguez, Solange Valdes, Mengmeng Niu, Abdulaziz M. Aldayel, Lan Peng, Stephen D. Hursting, and Zhengrong Cui

**Fig. S1.** (A)  $^1\text{H}$  NMR spectrum of DHA-dFdC (300 MHz,  $\text{THF-d}^4$ ). (B) LC/MS chromatogram of DHA-dFdC. (C) Mass spectra of DHA-dFdC. The LC/MS system used was an Agilent Technologies 6530 Accurate Mass Quadrupole TOF LC/MS using a RP C18 column (Agilent Zorbax, 50 x 2.1 mm, 5  $\mu\text{m}$ ) at 40°C. The mobile phase consisted of solvent A (water with 0.1% formic acid) and solvent B (acetonitrile with 0.1 % formic acid). Mobile phase composition was changed from 95% solvent A to 100% solvent B over 5 min, ran for 2 more minutes, and finally changed back to 95% solvent A over 4 more minutes. The flow rate was 0.7 ml/min. The target compound was detected at 4.85 min, and the compound was observed as  $[\text{M}+\text{H}]^+ m/z$  at 574.3,  $[\text{M}+\text{Na}]^+ m/z$  at 596.3,  $[2\text{M}+\text{H}]^+ m/z$  at 1147.6, and  $[2\text{M}+\text{Na}]^+ m/z$  at 1169.6.

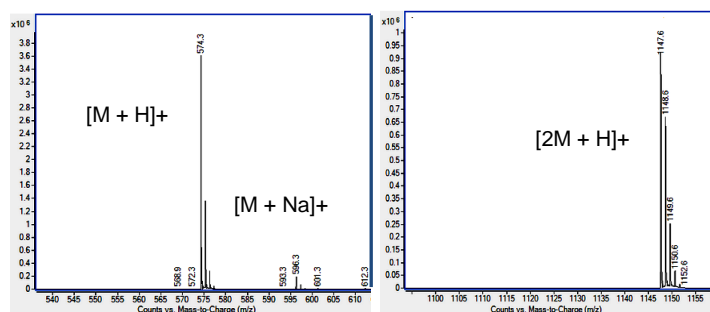
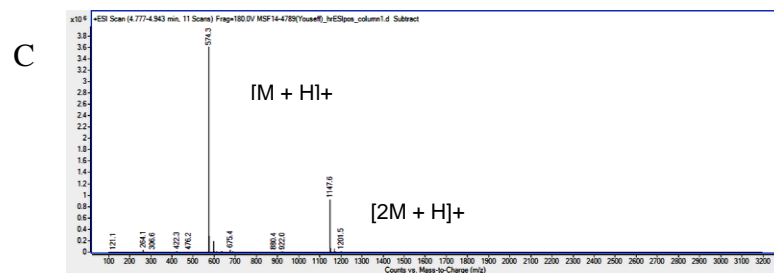
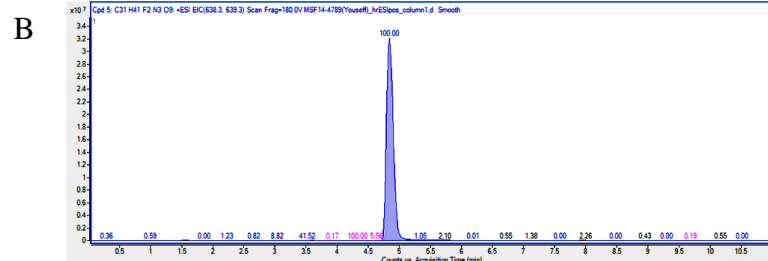
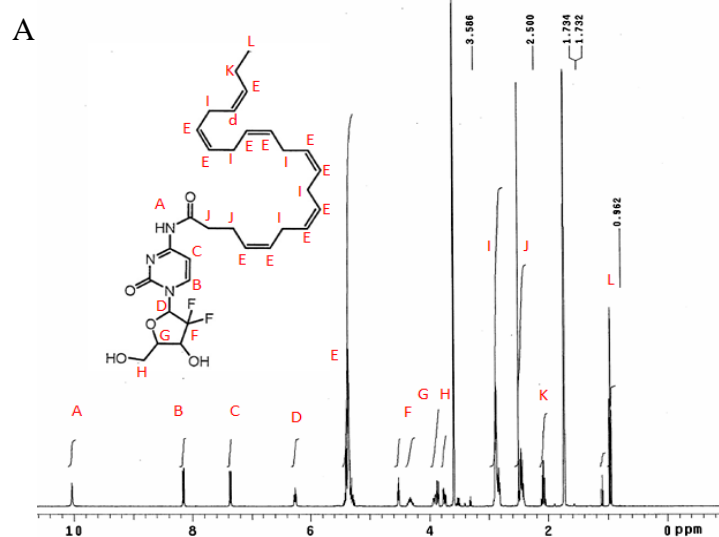


**Fig. S2.** A comparison of the  $GI_{50}$  values of DHA-dFdC and dFdC. Shown are the ratios of the  $GI_{50}$  values of dFdC vs. DHA-dFdC. Values larger than 1 indicate that DHA-dFdC was more cytotoxic than dFdC. Red bars represent cell lines in which the  $\log GI_{50}$  value of DHA-dFdC was less than -8.0.

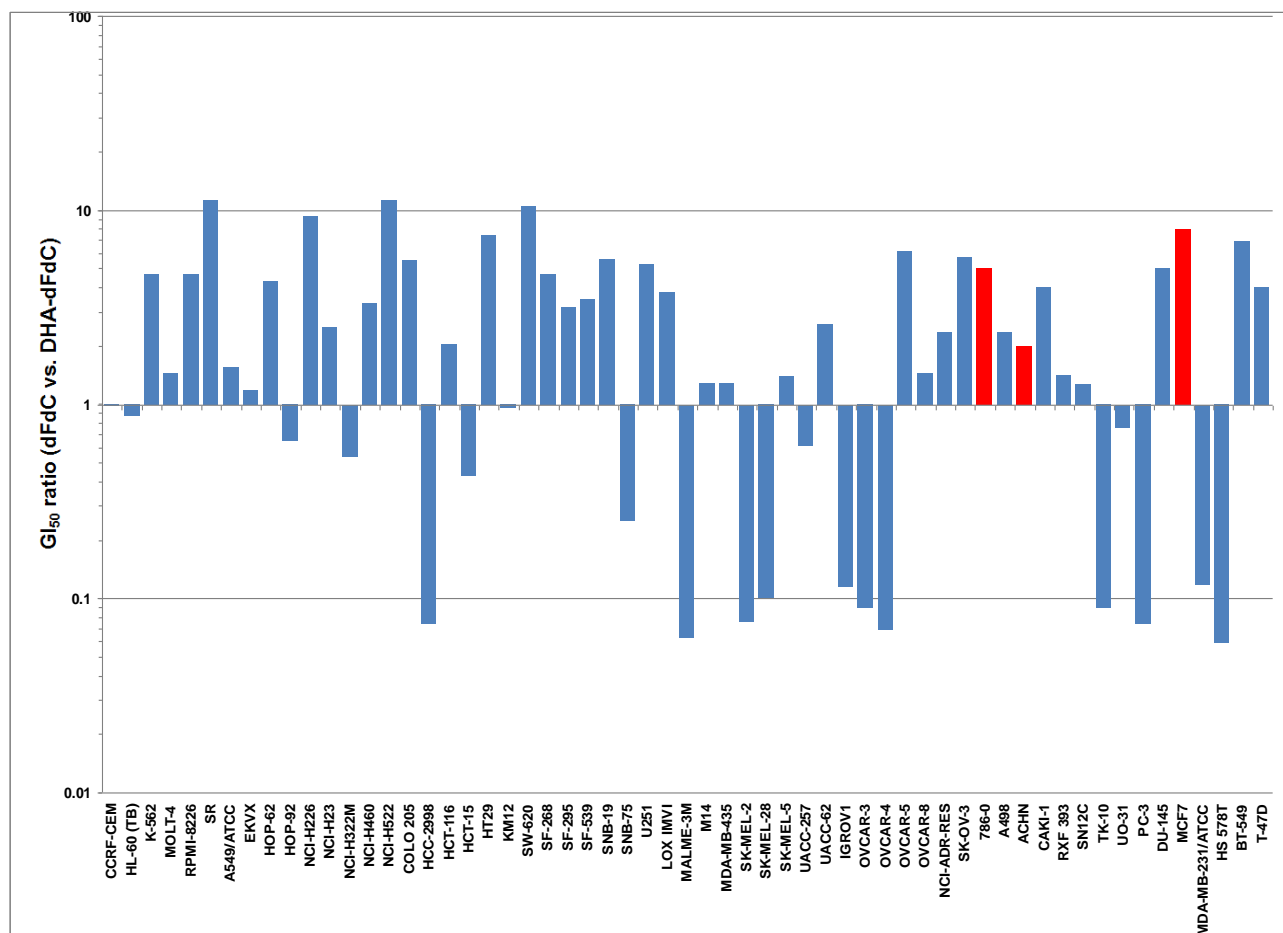


**Fig. S3.** Antitumor activity of DHA-dFdC against TC-1 cells in culture and in vivo. (A) Cytotoxic activity of DHA-dFdC against TC-1 murine lung cancer cells after 24 h of incubation. (B) TC-1 tumor growth curves following treatment with DHA-dFdC or dFdC. TC-1 tumor cells were s.c. implanted (500,000 cells/mouse) in the right flank of female C57BL/6 mice, and treatment started on the 7<sup>th</sup> day following tumor implantation. Mice received either DHA-dFdC in a Tween 80/ethanol/mannitol aqueous solution vehicle (50 mg/kg), dFdC in 5% mannitol solution (26.1 mg/kg), or were kept untreated. Treatments were given by i.p. injection, twice/week. (C) Mouse body weight during treatments. Data are means  $\pm$  S.D. (n = 5-6). (<sup>a</sup> p < 0.05, DHA-dFdC vs. other groups).

